Techno-economic analysis of coke oven gas and blast furnace gas to methanol process with carbon dioxide capture and utilization

Authors:

LINGYAN DENG DENG, Thomas Adams II

Date Submitted: 2020-01-09

Keywords: Economic and sensitivity analysis, methanol production, CO2 utilization and storage, blast furnace gas, COG desulphurization, Coke oven gas

Abstract:

This paper documents a process for converting coke oven gas (COG) and blast furnace gas (BFG) from steel refineries into methanol. Specifically, we propose the use of blast furnace gas (BFG) as an additional carbon source. The high CO2 and CO content of BFG make it a good carbon resource. In the proposed process, CO2 is recovered from the BFG and blended with H2O, H2, and CH4-rich COG to reform methane. Optimized amounts of H2O and CO2 are used to adjust the (H2 – CO2)/(CO + CO2) molar ratio in order to maximize the amount of methanol that is produced. In addition, the desulphurization process was modified to enable the removal of sulfur compounds, especially thiophene, from the COG. The process design and simulation results reported herein were then used to determine any potential environmental and economic benefits. This research is based on off-gas conditions provided by ArcelorMittal Dofasco, Hamilton, Ontario. In order to determine which conditions are most desirable for this retrofit strategy, potential greenhouse gas reduction and economic benefits were analyzed. In particular, this analysis focused on the heating utility chosen for methane reformation prior to methanol synthesis. To this end, COG, BFG, and natural gas (NG) were compared. The results showed that using BFG/NG as a heating utility can produce greater economic gains, and that synthesizing COG+BFG to methanol results in greater economic and environmental gains than solely producing electricity (the status quo). Compared to current operating procedures, the proposed process could potentially increase net present values by up to $21 million. The carbon efficiency achieved was up to 72.4 %. An additional 0.28 kg of CO2 is needed for every 1 kg of MeOH produced. About 52 % of feedstock energy is converted to MeOH, with another 33 % recovered in the form of utilities. The exergy efficiency of the recommended version of the system is about 62%. The business case for converting CO2 into methanol highly depends on the local electricity grid carbon intensity. For Ontario, it can reduce direct CO2 emissions by 189 ktonne per year, and fix up to 2,970 ktonne CO2 into methanol per year. However for China, this retrofit will result in additional CO2 emission of about 30 ktonne per year. In addition, analyses of location effects, CO2 taxes, electricity prices, electricity carbon intensity, methanol prices, and income taxes indicated that MeOH production is highly recommended for Ontario, Mexico, and China applications. In contrast, investment in this retrofitting procedure is not recommended for the USA and Finland. Aspen Plus Simulation files and other source code have been open-sourced and are available to the reader.

Record Type: Preprint

Submitted To: LAPSE (Living Archive for Process Systems Engineering)

Citation (overall record, always the latest version):	LAPSE:2020.0072
Citation (this specific file, latest version):	LAPSE:2020.0072-1
Citation (this specific file, this version):	LAPSE:2020.0072-1v1

DOI of Published Version: https://doi.org/https%3A//doi.org/10.1016/j.enconman.2019.112315

Design and Optimization of Coke Oven Gas and Blast Furnace Gas to Methanol Process with Carbon Dioxide Capture and Utilization

Lingyan Deng and Thomas A. Adams II*

Department of Chemical Engineering, McMaster University, 1280 Main St. West, Hamilton, Ontario L8S 4L7, Canada

**Corresponding author. Tel.:+1 905 525 9140 ext.24782 E-Mail address: tadams@mcmaster.ca*

Abstract

This paper documents a process for converting coke oven gas (COG) and blast furnace gas (BFG) from steel refineries into methanol. Specifically, we propose the use of blast furnace gas (BFG) as an additional carbon source. The high CO_2 and CO content of BFG make it a good carbon resource. In the proposed process, CO_2 is recovered from the BFG and blended with H_2O, H_2, and CH_4-rich COG to reform methane. Optimized amounts of H_2O and CO_2 are used to adjust the $(H_2 - CO_2)/(CO + CO_2)$ molar ratio in order to maximize the amount of methanol that is produced. In addition, the desulphurization process was modified to enable the removal of sulfur compounds, especially thiophene, from the COG. The process design and simulation results reported herein were then used to determine any potential environmental and economic benefits. This research is based on off-gas conditions provided by ArcelorMittal Dofasco, Hamilton, Ontario. In order to determine which conditions are most desirable for this retrofit strategy, potential greenhouse gas reduction and economic benefits were analyzed. In particular, this analysis focused on the heating utility chosen for methane reformation prior to methanol synthesis. To this end, COG, BFG, and natural gas (NG) were compared. The results showed that using BFG/NG as a heating utility can produce greater economic gains, and that synthesizing COG+BFG to methanol results in greater economic and environmental gains than solely producing electricity (the status quo). Compared to current operating procedures, the proposed process could potentially increase net present values by up to $21 million. The carbon efficiency achieved was up to 72.4 %. An additional 0.28 kg of CO_2 is needed for every 1 kg of MeOH produced. About 52 % of feedstock energy is converted to MeOH, with another 33 % recovered in the form of utilities. The exergy efficiency of the recommended version of the system is about 62%. The business case for converting CO_2 into methanol highly depends on the local electricity grid carbon intensity. For Ontario, it can reduce direct CO_2 emissions by 189 ktonne per year, and fix up to 2,970 ktonne CO_2 into methanol per year. However for China, this retrofit will result in additional CO_2 emission of about 30 ktonne per year. In addition, analyses of location effects, CO_2 taxes, electricity prices, electricity carbon intensity, methanol prices, and income taxes indicated that MeOH production is highly recommended for Ontario, Mexico, and China applications. In contrast, investment in this retrofitting procedure is not recommended for the USA and Finland. Aspen Plus Simulation files and other source code have been open-sourced and are available to the reader.

Keywords: Coke oven gas, blast furnace gas, COG desulphurization, CO_2 utilization and storage, economic and sensitivity analysis, methanol production.

1. Introduction

In steel manufacturing, there are three major by-product off-gases: coke oven gas (COG), blast furnace gas (BFG), and basic oxygen furnace gas (BOFG). These gases mainly contain CH_4, CO, CO_2, H_2, and N_2. When these off-gases are combusted, large amounts of CO_2 are directly emitted to the atmosphere. Indeed, according to the World Steel Association [1], the average CO_2 emission rate is 1.9 tonnes for every tonne of crude steel cast. This figure is significant, as direct emissions from the steel industry contribute to about 7% of all anthropogenic CO_2 emissions [2]. However, CO_2 emissions can be reduced by improving the efficiency of the steelmaking process via different technologies or by upgrading how these off-gases are utilized.

For example, the Ultra-Low Carbon Dioxide Steelmaking (ULCOS) initiative aims to reduce CO_2 emissions by 50%, and its four selected breakthrough technologies have been achieving some progress towards this goal. The first of these technologies is a top-gas-recycling blast furnace that is equipped with a process designed to capture and store CO_2 (CCS). The CO_2 removed from the BFG is recycled as reduction agent, while pure O_2 is used as an oxidant, thus removing unwanted N_2 from the air and making it easier to separate and capture CO_2 downstream. The second new technology is HIsarna, which also features a CCS process. This method consists of a reactor for coal preheating and partial pyrolysis, a melting cyclone for ore melting, and a smelter vessel for final ore reduction and iron production. This method requires the use of significantly less coal, and it is flexible insofar as it allows coal to be partially substituted with biomass, natural gas (NG), or even H_2. The third technology is ULCORED with CCS, which uses gases from the partial oxidation of NG instead of coal or coke. The direct reduction of iron ore is then transferred to the electric arc furnace (EAF) for steelmaking. Finally, the fourth technology is the low

temperature (about 110°C) iron electrowinning process. Instead of using coal or carbon compounds as reduction agents, this technology uses electrons and electrolytes to reduce the iron ore. Although electrowinning processes have the potential for zero CO_2 emissions, even without CCS, they are difficult to scale up.

These four options aim to reduce CO_2 emissions through new steelmaking technologies, but there is still a long way to go. The first three all require CCS, which can be practically impossible as steel refineries would need to be co-located near CO_2 sequestration sites and CO_2 pipelines would need to be constructed. The fourth technology though could achieve low CO_2 emissions without requiring CCS, but scaling-up to industrial size remains a major challenge. Hence this work focuses on other options for by-product off-gas valorization that are scalable, retrofittable, and do not require CCS. Throughout most of the steel manufacturing industry, COG is combusted for steam generation, which is subsequently used either for electricity generation using a low pressure steam turbine or as heat source. Deng and Adams [3] demonstrated that it is possible to retrofit the process by upgrading a COG-based low-pressure steam turbine system—which is a system present in many existing plants that combusts waste COG for steam generation—to allow it to function as a combined-cycle power plant (CCPP) to produce more electricity. Although this approach produces the same amount of direct CO_2 emissions, it can significantly reduce the amount of indirect CO_2 emissions because it requires less electricity to be purchased from the grid. Depending on the carbon intensity of the local power grid, this approach can reduce indirect CO_2 emissions by anywhere between 83.5 and 2221.1 $gCO_2e/kgCOG$. However, as the same authors have previously estimated [4], using COG to synthesize methanol (MeOH) instead of producing electricity may be an even more effective approach for reducing CO_2 emissions. In fact, researchers [5], [6] are studying the potential of fixing CO_2 into MeOH as a method of CO_2 mitigation. Pérez-Fortes et al. [5] studied the techno-economic and environmental feasibility of using H_2 and CO_2 recovered from pulverized coal power plants as raw material for MeOH synthesis. Though it demonstrated a net CO_2 emission reduction, and has the potential of consuming 1.46 tonne CO_2/tonne MeOH, the high cost of the raw material prevents profitability. In this work, cheap raw materials are used instead, namely the by-products COG and BFG from steel manufacturing. It is a promising method with both CO_2 mitigation potential and profitability benefits for steel manufacturing. Therefore, this work will build upon these authors' previous work by conducting a techno-economic analysis of the COG+BFG to MeOH system.

A recent study by Kim et al. [7] examined the energy efficiency and economics of producing MeOH out of COG in a polygeneration system. In their study, MeOH was not the only expected product of the conventional COG to MeOH process; rather, heat, power, and MeOH were all proposed as being products of a single system. Significantly, the results showed that their approach increased energy efficiency from 38% to 53%. Furthermore, Kim et al. also analyzed MeOH's price trigger point. However, this analysis failed to demonstrate the effect of the carbon tax. Furthermore, their analysis underestimated desulphurization capital costs; they only considered H_2S removal due to the assumption that COG is purified and free of organic sulphur content. Moreover, it must be noted that, contrary to Kim et al.'s descriptions, the traditional COG to MeOH process does not separate H_2 out of COG via pressure swing adsorption (PSA) before steam methane reforming (SMR). The paper they cited [8] to support this claim actually says that the traditional H_2 recovery method (not for the purpose of producing MeOH out of COG) uses PSA to separate H_2 out of COG (A typical commercial method for converting COG to MeOH is shown in Figure 1). As can be seen, instead of consuming CO_2, this polygeneration process actually produces significant amounts of direct and indirect CO_2 emissions [7]. In contrast, the method detailed in this paper aims to achieve negative net CO_2 emissions by fixing the CO_2 to the maximized production of MeOH. This approach has considerable potential, as one of the key findings of Kim et al.'s study was that it is more economically beneficial to produce a maximum amount of MeOH rather than produce more electricity and heat, but less MeOH.

The preferred $(H_2-CO_2)/(CO+CO_2)$ molar ratio (R parameter) is 2.04 for MeOH production from syngas [9]. Since COG is rich in H_2 and CH_4, its H_2/CO molar ratio is around 8, which is much higher than preferred ratio. Although coal gasification is traditionally the source of additional carbon, some researches propose combusting half of COG for carbon source hence sacrifice the production of MeOH [10], this work proposed a process uses BFG as a carbon resource and maximize the production of MeOH. This idea is not new. Ghanbari et al. [11], [12] proposed a polygeneration system in which BFG, COG, and BOFG are used as raw materials to generate electricity, DME, and/or MeOH. However, their work assumes that COG is sulphur free, which means that the desulphurization process was not considered in their economic analysis. Given that thiophene's stability makes it rather difficult to remove from COG, it is likely that Ghanbari et al.'s economic analysis underestimated the cost. Traditionally, methane in COG is converted to H_2 and CO via steam methane reforming. However, under this process, a reverse water-gas shift (RWGS) is required to adjust the R parameter due to high H_2 content. In addition, the MeOH synthesis process is very sulfur sensitive. The catalyst used in the MeOH synthesis process can very easily be deactivated by sulfur compounds, with sulfur tolerances as low as 0.1 ppmv [13], [14]. The commercialized

desulphurization method is a two-stage hydrodesulphurization process [15], [16]. Wu [15] has also suggested using high-temperature non-catalyst partial oxidization (NCPO), as this approach is capable of cracking methane and thiophene at the same time. In contrast, other researchers [17], [18] have recently suggested using CO_2 dry reforming (CDR) directly for methane reforming, as this method could potentially shorten the COG to MeOH process by removing the RWGS process. Furthermore, due to the high temperature of CDR, thiophene could be converted to H_2S and then removed using a middle-temperature sulfur-removal process (MTSR). CDR is a promising technology due to its ability to convert methane, desulphurize thiophene, and adjust the R parameter; however, it requires high temperatures to mitigate the carbon deposition effect [18]. The combination of steam and CO_2 reforming (CSR) offers one viable method for increasing MeOH production and reducing the carbon deposition effect [19].

Therefore, we can conclude from the literature review that CSR is likely the best approach to create a process that reduces CO_2 emissions in steel refining and also does not require CCS. Moreover, the important individual components of the system are commercially available or technologically viable at scale, and so they can be used immediately without the need for further research to develop new materials or technologies (like electrowinning) at scale. These properties make it potentially the most commercially attractive option compared to the other four approaches because it has the fewest barriers to development. However, there are some key knowledge gaps in the literature that need to be overcome before the CSR approach can be commercialized, which we address in this work:

1. *Organic sulfur*. Some organic sulphur compounds present in COG present a major challenge for this process because they will poison downstream methanol synthesis catalysts. Thiophene is especially difficult to remove. All previous studies in the literature on COG to methanol have not considered this aspect of process synthesis. In this work, we specifically address this gap in thiophene considerations by presenting a novel desulfurization process that takes all of the forms of sulphur into account. Without this step, methanol synthesis could not be achieved practically.
2. *CO_2 utilization from BFG.* Previous studies looking at methanol synthesis through the CSR route have used CO_2 sources from outside the steel manufacturing process, such as coal combustion. However, our paper is the first to study the capture and utilization of CO_2 from elsewhere in the refinery, particularly from BFG. We also analyse how using BFG can impact the balance of plant because we are changing its makeup. This is important to address because sourcing large amounts of high-purity CO_2 from outside the refinery is not usually practical in most retrofit scenarios, and so this gap must be addressed to improve the chances of commercialization.
3. *Eco-Techno-economic analyses.* There is a major gap in the literature in terms of understanding and assessing the value of the CSR concept in terms of both economic and environmental objectives. In this work, we address this gap by a detailed analyses of a CSR retrofit, and we consider the application of this concept in five different geo-political regions because the economics and environmental impacts are strongly influenced by the local electricity grid, local market prices, and local carbon taxes. This knowledge gap is important to address because the decision whether to retrofit a steel refinery with the COG + BFG to MeOH process depends highly on these issues.

2. Methodology and Process Description

There are six main steps involved in producing MeOH with COG and BFG as raw materials: first, recover the CO_2 from the BFG; second, remove the sulphur compounds from the COG; third, mix the purified COG and CO_2 and convert them to methane in the CSR unit; fourth, adjust the R parameter and synthesize the MeOH; fifth, recycle most of the unconverted gas in order to increase production rate and purge the remaining unconverted gas to avoided inert gas accumulation; and finally, purify the MeOH. It is important to note that there may be overlap between these steps; for example, although it is responsible for removing thiophene from the COG, the CSR unit is also involved in converting methane. In addition, since the COG-sulphur-removal (mainly H_2S via Rectisol) process has already been commercialized, the related simulations have also been previously verified. As these simulations have shown, capital costs and operation costs are linearly related to the amount of H_2S that is removed [20]. Therefore, there is no further need to verify these simulations in this work. Furthermore, the kinetic equation used in the MeOH synthesis model has also been widely used and verified [21], [22]. The only aspect of the CSR process that requires verification is the methane conversion process, which is detailed in Section 2.2.1. To enhance readability, the following discussion will be organized based on the six steps outlined above. The final proposed MeOH synthesis process is shown in Figure 2.

2.1. Additional carbon resource from BFG

Among the three main off-gases produced in steel manufacturing, COG has the highest calorific value and a high H_2 content, while BFG has a low calorific value, but is generally produced in the largest volumes (about 14 times that of COG). The third off-gas, BOFG, is produced in batch mode and will not be considered in this particular paper. Traditional BFG consists of about 23 vol. % CO_2 and 22 vol. % CO, with the remainder mostly being made up of N_2. Detailed compositions of COG and BFG are shown in Table 1.

Table 1. COG and BFG compositions. * in PPMV. Source: [23], [24].

	HHV (MJ/kg)	T(°C)	P (bar)	Composition (vol.%)									
				C_2H_2	CH_4	CO	CO_2	H_2	N_2	O_2	H_2S*	CS_2*	C_4H_4S*
COG	22.6-32.6	35	1.45	1.5-3.0	22-28	5.0-9.0	1.0-3.5	45-60	3.0-6.0	0.1-1.0	3420-4140	72-102	20-40
BFG	2.6	28	1.44	-	-	23.5	21.6	3.7	46.6	0.6	-	-	-

BFG is usually combusted to produce low-grade heat for use in the steel manufacturing process, which results in very high CO_2 emissions. The proposed method is based on the idea that, rather than using CO_2 from coal gasification, it may be more effective to recover and use the CO_2 from the BFG for COG methane reforming and R parameter adjustment. There are three main techniques for separating CO_2 from BFG: pressure swing adsorption (PSA), membrane separation, and MEA absorption. A comparison of these techniques was conducted in order to identify the most suitable method for use in our proposed COG+BFG to MeOH process. This comparison process is detailed in the following sub-sections.

2.1.1. PSA technology to separate CO_2 from BFG

Pressure swing adsorption (PSA), or vacuum pressure swing adsorption, is one approach that is routinely used to upgrade BFG. This method works by removing the CO_2 from the BFG and then recycling the CO_2-depleted BFG back into the blast furnace [25], [26]. The Linde Group has developed a PSA system that features a unit capacity of up to 300,000 Nm^3/h and the ability to achieve a product purity of 95 vol. % [27]. The pressure used in their PSA ranges from 7 bar to 35 bar, with a minimum CO_2 feed-gas content of around 10 vol%. According to the literature [28], [29], the estimated cost of recovering the CO_2 from BFG containing 30–40% CO_2 and 10-20% N_2 is approximately \$38/ton (\$41.9/tonne) CO_2 (all dollar values in this paper are expressed in US \$). This figure includes the cost of compressing the CO_2 to 120 bar. The cost in this study should be relatively lower than \$38/ton (\$41.9/tonne) CO_2 because the CO_2 recovered will be used directly for CSR without requiring compression. By comparison, the JFE steel developing PSA process, which uses zeolite as an adsorbent, costs \$41/ton (\$45.2 /tonne) CO_2 [30]. However, JFE's process is capable of purities as high as 99% [30].

2.1.2. MEA technology to separate CO_2 from BFG

Chemical absorption technology is the most mature commercialized technology for CO_2 capture, especially for NG and syngas sweetening. However, the two main drawbacks to these approaches are their high rate of equipment corrosion—specifically amine degradation by O_2, hence their higher absorbent makeup rates—and their high energy costs, which is due to the high temperature required for absorbent regeneration [29]. The regeneration of monoethanolamine (MEA) during the stripper process usually accounts 70-80% of the CO_2 extraction process' entire operating costs [31]. Nonetheless, MEA has been demonstrated to be a good choice for separating CO_2 from gases [32], as it favors higher pressures and lower temperatures (35–50 °C) for CO_2 absorption and lower pressures and higher temperatures (around 120 °C) for CO_2 desorption in the stripper. MEA has also demonstrated high absorption and CO_2 production rates for BFG's specific gas composition, which contains higher concentrations of CO and H_2 than traditional post-combustion flue gas [33]. The use of MEA absorption can produce recovery rates ranging from 67.8% to 98.4% due to different concentrations of MEA in solution [34]. Separation costs are approximately \$71.7/ton (ton=2000 lbs) (\$79.0/tonne, tonne=1000 kg) CO_2 when using BFG containing 30-40% CO_2 [29].

2.1.3. Membrane technology to separate CO_2 from BFG

The main advantages of membrane technologies are their low capital investment, good space efficiency, ability to be scaled-up, minimal associated hardware, flexibility, and minimum utility requirements [35]. On the other

hand, they also have a few disadvantages, including the need for clean feed (particulates and, in most cases, entrained liquids must be removed) [35], and a tradeoff between permeance and selectivity, which can make it difficult to achieve both high yield and high purity vis-à-vis the recovered products from a systems perspective. Permeance and selectivity are particularly important for BFG. A simulation based on a binary gas (ideal) mixture (CO_2 with one of BFG's other constituent gases, i.e., H_2, N_2, or CO) revealed an estimated total CO_2 recovery cost, including the cost of CO_2 compressed to 110 bar, ranging between 15.0 and 17.5€/tonnes CO_2 (18.1 to 21.1$/tonne CO_2) [30]. However, the cost of recovering CO_2 from the BFG real mixture was not documented in this paper [30]. A more relevant study by Ramírez-Santos et al.[36] found that a commercialized industrial-scale blast furnace flue gas membrane separation process (from MTR Inc.) was able to recover up to 90% CO_2 with 95% purity and a cost range of 23 to 33€/ton CO_2 (28.2 to 40.5$/tonne CO_2).

The above three methods have all been commercialized. For the purposes of our study, we assume that the cost estimates of the aforementioned studies are directly comparable (i.e., that they have similar enough assumptions, boundary definitions, conditions, and methods) and can be taken at face value such that the cost of CO_2 recovery increases in the order of membrane, PSA, and MEA recovery methods. Since the purity and recovery rate are not a primary focus in this study, the relatively higher purity obtainable via MEA or PSA is not necessary from a systems perspective. Hence, the membrane method was selected for CO_2 recovery, as it appeared to meet the process needs at the lowest cost when taking the reported costs in the literature at face value.

2.2. Methane reforming

2.2.1. Methane conversion process validation

In the third step of the process, the recovered CO_2 and the sweetened COG are fed into a methane-reforming reactor, which is placed inside a furnace and maintained at a high temperature. In the reformer, the methane in the COG is reformed into synthesis gas, and the thiophene and carbon sulfide in the COG is reformed into H_2S; this process has been demonstrated at this temperature at the lab scale by Zhang et al. [37] and Cao et al. [17]. Zhang et al. [37] used a CDR reactor, which is a continuous-flow quartz reactor that is packed with a coal char catalyst, and a mixed-gas residence time of 3 seconds. A platinum-rhodium thermocouple is installed in the centre of the catalyst bed to detect the temperature, which is increased up to a maximum temperature of 1200 °C using electricity. However, quartz-flow reactors are not traditionally used in industrial applications; rather, stainless steel furnaces are most commonly used in these settings. Specifically, stainless steel 310 is optimal for constructing furnaces due to its very high temperature rating and ability to withstand temperatures of up to 1100 °C. The CDR process has a higher methane conversion rate than NG + CO_2 dry reforming due to its high H_2 content. The proposed method enables CDR to achieve up to 100% methane reformation at high temperatures (1100 °C), without being significantly affected by the carbon formation phenomenon. Indeed, the conversion rate is much higher than the NG + CO_2 dry reforming method, which achieves nearly 90 % methane conversion [38] but has a significant carbonation effect.

The CDR was modeled using the RGIBBS reactor module in Aspen Plus (which assumes both chemical and phase equilibria are achieved), with the results showing that the organic sulfur was almost entirely converted to H_2S. To validate the RGIBBS model, the simulation conditions were set to the exact same gas composition, operation pressure, and temperatures used in [39]. As such, the CDR experiment was conducted at temperatures of 800 °C, 900 °C, and 1000 °C with a Ni/γAl_2O_3 catalyst (with 5 wt. % Ni) in a fixed-bed quartz reactor under atmospheric pressure. The volumetric hourly space velocity (VHSV) was 0.75 liter gas per gram of catalyst per hour (L g^{-1} h^{-1}) and was adjusted by adding or reducing the amount of catalyst. The results showed that that the conversion rate was highest at the lowest used VHSV, which was 0.75 L g^{-1} h^{-1}. Thus, in this study, a VHSV of 0.75 L g^{-1} h^{-1} will be used. Furthermore, the experiment defined the gas composition as 54% H_2, 23% CH_4, and 23% CO_2 (GTM), but neglected other components, such as H_2O, N_2, C_2H_2, and C_2H_6, among others. Their experiment reached equilibrium within 60 minutes. As temperature increased, the equilibrium time decreased from around 70 minutes to 20 minutes. The comparison of the CH_4 and CO_2 conversion is detailed in Table 2.

Table 2. Validation of CDR simulation using RGIBBS model

	Experiment conversion rate (%) [39]		RGIBBS conversion rate (%)		Error (%)	
	CO_2	CH_4	CO_2	CH_4	CO_2	CH_4
800 °C	95	85	93.2	88.25	-1.89	3.82

900 °C	96.9	95.6	98.32	94.838	1.465	-0.80
1000 °C	100	100	99.51	97.64	-0.49	-2.36

As Table 2 indicates, the error between the experimental results and the Aspen Plus simulation results was less than 4% for all of the three different temperature cases. This is an acceptable level of error for a first stage techno-economic analysis. In addition, the CH_4 and CO_2 conversion rates from the RGIBBS model were slightly lower than those observed in the experiment, meaning the simulation results will be on the whole more conservative. The exceptions to this trend were the CH_4 conversion rate at 800 °C and the CO_2 conversion rate at 900 °C. Overall, the results suggest that RGIBBS can be used to simulate the CDR process.

Carbon deposition happens at low temperatures in the CDR process, and the CH_4 conversion rate is lower at the relatively low temperature of 800 °C. As such, some researchers might argue that CDR at high temperatures could achieve up to 100% CH_4 conversion. However, achieving these extremely high temperatures (1000 °C) would require more expensive reactor material. As such, Koo et al. [40] studied the viability of using combined CO_2 and steam reforming (CSR) of methane in COG. Their results demonstrated that high CH_4 conversion can be achieved by using a Ca-promoted $10Ni/MgAl_2O_4$ catalyst for COG reforming, and that this approach offers superior coke formation resistance to those that do not use a Ca addition. Specifically, the CH_4 conversion rates ranged from 83.7% to 91.3% at 900 °C, with a fixed CH_4: H_2O: CO_2: H_2: CO: N_2 mole ratio of 1: 1.2: 0.4: 2: 0.3: 0.3, respectively. However, they did not study the composition effects on the conversion. Jang et al. [19] examined whether the CSR of methane effectively reduces carbon deposition when the mole ratio of $(CO_2+H_2O)/CH_4$ is higher than 1.2 and Ni-MgO-$Ce_{0.8}Zr_{0.2}O_2$ is used as a catalyst. Their results indicated that the CH_4 conversion rate could reach up to 99.8% at 800 °C and a $(CO_2+H_2O)/CH_4$ mole ratio of 2.9, which they confirmed using a Gibbs free energy minimization based equilibrium simulation (the same idea as an RGIBBS model in Aspen Plus). The RGIBBS model based CH_4 conversion rate in this work is 97.8 % with $(CO_2+H_2O)/CH_4$ mole ratio of 2.8 at 800 °C. This rate is a little bit lower than those documented in the literature due to the relatively lower $(CO_2+H_2O)/CH_4$ mole ratio. Hence, the use of RGIBBS in Aspen Plus can be considered representative for CSR simulations.

2.2.2. CSR heating utility chosen

In this process, the CSR unit requires the largest amount of heat possible, and there are two obvious continuous energy sources that can be used to satisfy this need: BFG and COG. Another conventional material that can be used to generate heat is NG. In addition, the purge stream (PURGE1 in Figure 2) could also be a potential heating utility given the considerable amount of energy it contains. However, since the pressure of the purge stream is very high, it was decided that it would be much better to generate power using a gas turbine instead of simply releasing the pressure without energy recovery and combusting it to provide heat for the CSR process.

BFG has a very low heating value. Therefore, before using it as a heating utility for CSR, it is crucial to ensure that the BFG can be combusted at temperatures greater than 800 °C in order to heat the CSR. A study by Ji-Won Moon et al. [41] also demonstrated that BFG combustion could reach up to 1193 °C under stoichiometric conditions. For comparison purposes, BFG, COG, and NG combustion were simulated in Aspen Plus using the RSTOIC combustion model and 20% more air than in the stoichiometric condition is provided. Table 3 shows that combustion temperature of all three gases are very high. The BFG combustion temperature is higher in the present study due to the use of a slightly higher air/BFG input temperature and its slightly higher HHV. Nonetheless, it is safe to say that NG, BFG, and COG are qualified heating utility candidates for a CSR unit.

Table 3. CSR utility comparison

	High heating value (MJ/kg)	Temperature of combustion at 20% excess air (°C)	Price ($/GJ)	Flow rate (kg/kg COG)	CO_2 emission factor (kg/kJ)
BFG	2.64	1269	0	3.12	247.90
COG	32.53	1991	0	0.20	36.01
NG	55.57	1825	1.61	0.15	49.59

However, the use of each utility affects certain variables, such as the production rate of MeOH, the reduction of direct CO_2 emissions, and the operation costs. The following compares the relative benefits and drawbacks associated with each heating utility:

a. NG

Natural gas has a higher heating value than BFG and COG. If heating is provided by combusted NG, then H_2-rich COG can be used completely for methanol synthesis, while BFG could still be used further downstream in the steel manufacturing process to provide heat for things like galvanizing. In addition, the use of NG would achieve the highest level of MeOH production, as it would provide enough heat to convert all of the COG. The drawbacks to using NG as a heating source is that there would be utility costs and increased fossil fuel consumption associated with its use.

b. COG

COG has a moderate HHV. If the raw COG is free, the utility cost for this CSR unit would be zero. Although COG is originally used to generate electricity, the amount it generates is ultimately replaced by electricity purchased from the market. In this case, about 20% of the COG will be required to heat up the CSR unit, while the remaining 80% will be used for MeOH synthesis. The use of COG as a heating utility will result in the lowest CO_2 emissions of the three heating utilities (Table 3), and it also has the lowest capital costs, operation costs, and utility costs due to the relatively smaller amounts required. However, the use of COG will reduce MeOH production by about 20% compared to NG/BFG. Since it is not obvious whether the use of COG as a heating utility provides significant benefits, further detailed calculations are computed in later sections.

c. BFG

BFG has a very low HHV compared to NG and COG, and it produces the highest CO_2 emissions when used for CSR heating. In addition, if BFG is used as a heating utility for CSR, it becomes necessary to find another heating source to replace it for downstream steel manufacturing. Therefore, any calculations of CO_2 emissions associated with BFG must also take into account the CO_2 produced by this additional heating source. For example, if NG is used in downstream to replace the BFG being used for CSR, the utility cost and MeOH production rate would be the same as just using NG for CSR in the first place. On the other hand, if BFG is considered a free heating source, and its use will not affect the downstream process, then the utility cost for the CSR unit would be zero. However, the use of BFG may lead to higher CO_2 emissions than the use of COG. Conversely, if BFG's replacement in the downstream process is less carbon intense and has a lower utility cost than NG, then BFG might be a cheaper and more environmental friendly option than NG.

Since it is not obvious whether COG is the best available heating utility, a thorough comparison is needed. This comparison is provided in Sections 3.2 and 3.3, wherein the system design and optimization, TCI, and TOPC, among other features, are compared in detail.

2.3. COG desulphurization

The conditions required for MeOH synthesis are stringent, especially regarding catalyst deactivation due to sulphur compounds. Thus, it is important to remove sulphur compounds from COG-converted syngas. Commercialized plants have found that, as a rule, the total concentration of sulphur compounds in syngas should be less than 0.1 ppmv [16], [42]. In general, the COG emitted from coke ovens is high in H_2S, COS, CS_2, and C_4H_4S. Fortunately, there are numerous available technologies for removing H_2S, COS, and CS_2 that are already very mature. For example, physical adsorption, chemical absorption, and wet oxidization are commonly employed to remove H_2S. However, it is much more difficult to remove C_4H_4S using these methods, largely due to being a stable heterocyclic compound. As such, the commercial desulphurization process is very complicated. A representative commercialized method is shown in Figure 1.

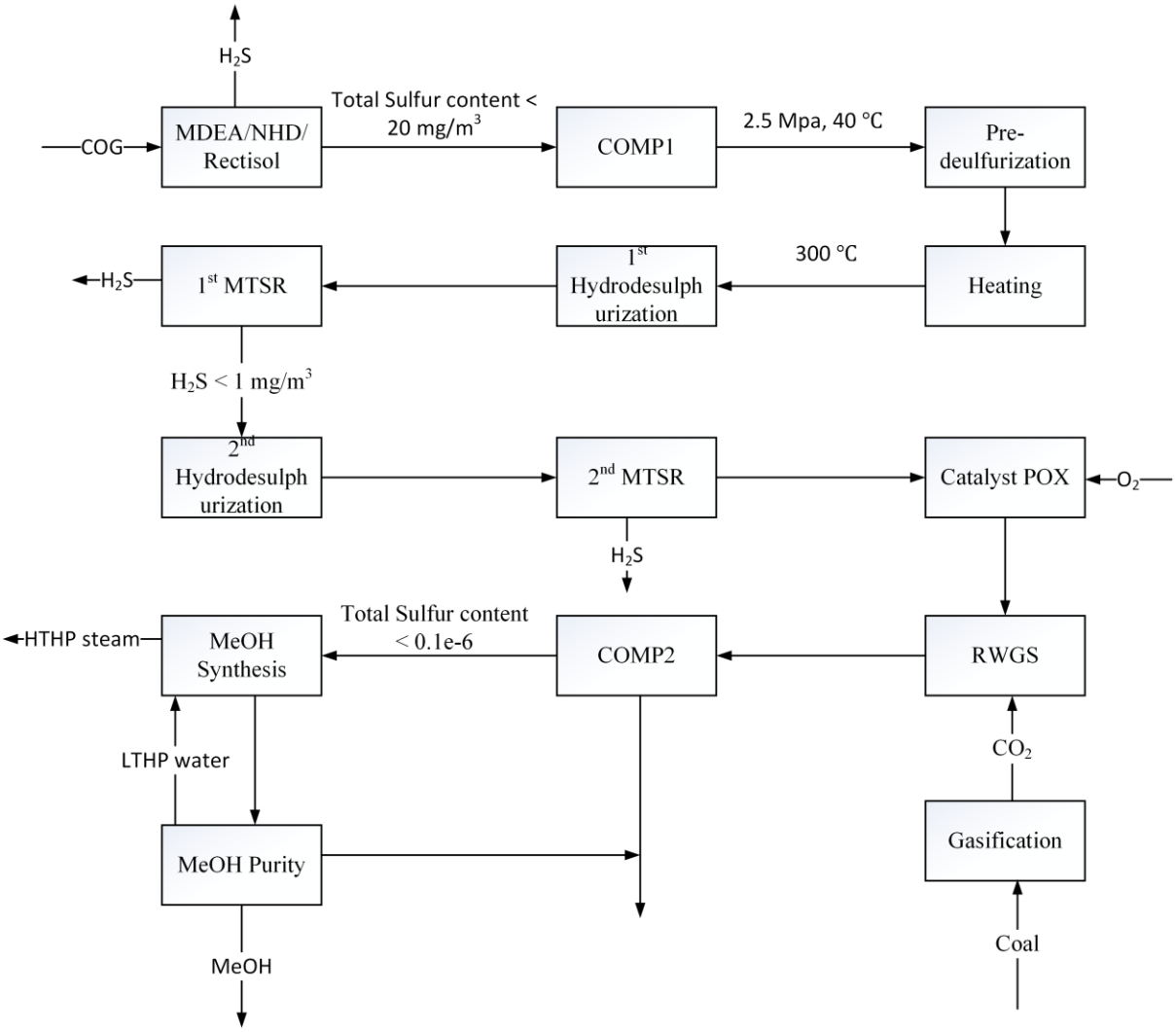

Figure 1. Typical commercialized COG to MeOH process (Ref.: [16])

As Figure 1 shows, the high H_2S content in the COG is mostly removed via wet desulphurization, which reduces the total sulphur content to less than 20 mg/N^3. Next, the COG is compressed to 2.5 MPa and heated up to 300 °C in order to conduct the first stage of hydrodesulfurization, which mainly converts organic sulphur compounds to H_2S. At the same time, unsaturated hydrocarbons (HC_A) are also converted to saturated hydrocarbons. After this stage, a catalyst is used to further reduce the converted H_2S to less than 1mg/N^3. Following this step, a relatively more expensive catalyst is used to conduct a second stage of hydrodesulfurization wherein the remaining organic sulphur compounds (especially C_4H_4S) are converted to H_2S and unsaturated HC_A is converted to saturated HC_As. The most expensive ZnO catalyst is used in the last desulphurization stage to ensure that the concentration of sulphur compounds in the gas is less than 0.1 PPMV. The CH_4 in the COG is then reformed into H_2 and CO using a catalyst partial oxidization unit, with CO_2 from coal gasification being added to the process to adjust the H_2/CO mole ratio. At last, the syngas is converted into MeOH using the typical catalyst, pressure, and temperature.

In this paper, a shorter and more effective desulphurization method is proposed, namely, CDR/CSR. This method allows both methane and organic sulphur compounds to be converted at the same time, while also minimizing the carbon formation/catalyst deactivation effect. As Bermúdez et al. [39] noted, Ni/γAl_2O_3 is used as a catalyst during CDR. Al_2O_3 is mainly used as a support, and the catalyst effect is mainly provided by the metal, in this case, Ni. Catalyst deactivation largely occurs due to carbon deposits created by methane decomposition, which can block the reactants' access to the active center, while another common cause is the sintering of nickel particles on the catalyst surface [39]. It is believed [43], [44] that hydrocarbons dissociate to produce highly reactive monatomic carbon on the surface of the nickel-based catalyst; once the gasification of the monatomic carbon rate becomes lower than its formation, the excess monatomic carbon will grow and form nickel carbide (the growth of carbon whiskers). However, if the gas contains H_2S, carbon whiskers will not grow because the H_2S will adsorb in the

nickel surface. Trimm [43] and Rostrup-Nielsen [44] both attempted to determine how much H_2S is needed to prevent carbon deposit. Each found that carbon formation remained close to the equilibrium point when (H_2S/H_2) was in the range of 0.5 to 27 × 10^{-6}, with few normal carbon whiskers being observed at H_2S/H_2 at 0.5 × 10^{-6}. Although carbon formation can be inhibited by increasing the H_2S content in the gas, excessive levels of H_2S can also deactivate the catalyst by occupying the hollow site on Ni.

While a different catalyst is used for CSR in this work, Ni is still responsible for producing the main catalyst effect. Consequently, it is reasonable to expect that H_2S will have the same effect on a Ni-MgO-$Ce_{0.8}Zr_{0.2}O_2$ catalyst. In addition, Rectisol is used to reduce the levels of the H_2S and COS (if any) in the COG to lower than 0.1 ppmv [45], while the organic sulphur in the sweet COG is converted to H_2S during the CSR with the nickel catalyst [46]. The H_2S/H_2 ratio is less than 27 × 10^{-6}, which means that catalyst deactivation can be restricted. Thus, this process enables hydrodesulfurization and the various stages of catalytic H_2S removal to be shortened to one middle-temperature Fe_2O_3 catalytic H_2S removal step after CSR. Furthermore, the MeOH production process can also be shortened, as shown in the design depicted in Figure 2.

2.4. MeOH synthesis and composition effect

Various experiments using mature MeOH synthesis processes have shown that H_2O will be produced during MeOH synthesis when it is absent in the feed gas [47]. Conversely, the production or consumption of CO_2 is entirely dependent on the composition of the syngas [22]. In the case of the pure H_2 and CO used for methanol synthesis, water is needed to initiate the reaction and to enhance the methanol synthesis rate. However, the final MeOH production rate can be inhibited if the water content in the syngas is increased too much [48]. In contrast, the H_2O and the MeOH production rate increase alongside CO_2 [47]. It is commonly believed that a CO_2/H_2 mixture will facilitate a decent rate of MeOH synthesis, while a CO/H_2 mixture will produce a very slow rate of synthesis. Thus, either CO_2 or H_2O needs to be added to the syngas.

Water-gas shift (WGS) has proven to be an effective method for adjusting the R parameter in order to maximize MeOH production. Specifically, an R parameter of 2.04 is optimal for MeOH synthesis [9]. There are two types of WGS: high-temperature WGS and low-temperature WGS [47]. The equilibrium constant for WGS increases as temperature decreases. In this paper, low-temperature WGS is needed to enhance the forward WGS, and a CO_2 removal step is also required to remove excess CO_2 in order to achieve an optimal R ratio [49]. However, the above-described CSR process allows the R parameter to be adjusted by changing the ratios among the CO_2, CH_4, and H_2O in the CSR unit, which eliminates the need for WGS.

2.5. System design and optimization

According to the above discussion, two design choices are possible: one that utilizes WGS/RWGS, as shown in Appendix *Figure A1*; and another that does not use WGS/RWGS, as shown in *Figure 2*. Both designs are modeled

in Aspen Plus v10 using the PR-BM physical property package for the gas-related units and STEAMNBS for all water streams/operations.

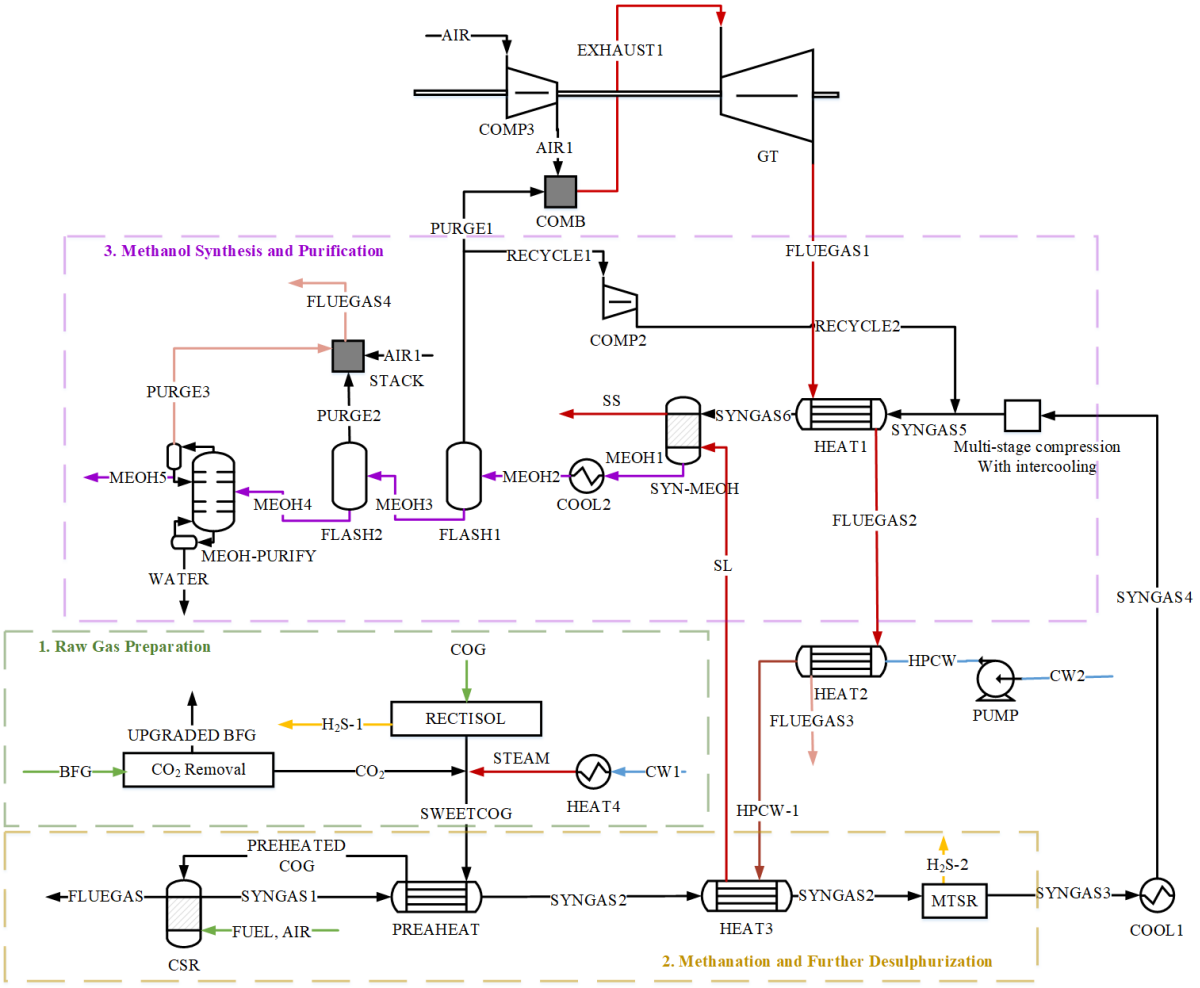

Figure 2. The proposed COG + BFG to methanol process using CSR for methane reforming and organic sulfur handling

As described above, the additional CO_2 is recovered from BFG, and the COG is sweetened via the Rectisol process to remove H_2S. The mixture of sweet COG, steam, and CO_2 is then injected into the CSR reactor, where methane and organic sulphur are converted into H_2S. The syngas from CSR is in turn used to preheat the raw gas mixture. Next, the syngas, which is still at a high temperature, must be cooled to 300 °C for the H_2S removal process. At the same time, the high-pressure water, which is used as a coolant for methanol synthesis, has to be heated to 240 °C. Thus, there may be heat exchange between these two streams, though the heat from the syngas stream is not great enough to heat the coolant to the required temperature. To remedy this, additional heat can be provided by the flue gas that is emitted from the gas turbine. The reactor effluent is then cooled to 300 °C and used in the adsorbent-based middle-temperature sulfur-removal (MTSR) process. Fe_2O_3 is used as a catalyst in the MTSR unit. Furthermore, a ZnO catalyst-based middle-temperature H_2S removal unit is also used to make sure that the H_2S content in the syngas is less than 0.1 PPMV [16]. The H_2S can be further processed to produce solid sulphur via a commercialized Claus process. However, this is outside the scope of this research.

The cleaned syngas is then cooled and fed into a multistage compressor to be compressed to 52 bar. The kinetic functions for MeOH synthesis are partial-pressure based [21]; that is, higher pressure is preferred to lower pressure. However, the use of pressures that are too high will result in high capital costs for the compressors and high utility costs for electricity. The pressure effect has been widely studied [21], [22], and this study uses pressures that are consistent with those used in the commercialized MeOH synthesis process [21]. Furthermore, compressor efficiency (0.72) is set to the default, and air is used as the inter-stage coolant. After further temperature adjustment, the syngas is fed into the MeOH synthesis unit, which is temperature controlled using boiling water. The methanol synthesis unit (SYN-MEOH) uses the RPLUG model and features a reactor with co-current thermal fluid. A design spec specifies the input coolant (high-pressure water) amount, which restricts

phase changes to those via evaporation in order to maintain the reactor's temperature. The MeOH synthesis kinetics were taken from Abrol et al. [21]. The product is cooled and flashed, with some of the unconverted gas being recycled back into the synthesis unit and the remainder being purged for combustion in order to avoid accumulation (such as the inert N_2). The purged gas (PURGE1) is combusted with air that has been compressed to an identical pressure, which is controlled by a calculator block. In addition, the gas turbine's maximum temperature is controlled to 1260 °C [3] by adding excess air. The heat in the flue gas out of gas turbine is used to heat the high-pressure water to be used in the boiling-water shell-and-tube MeOH synthesis unit. The product stream is further flashed and distilled to achieve the desired purity (98 wt.%) via the design specs. The unconverted gas from the second flash drum is then combusted, and the heat from this combustion is used to generate steam utility. The key stream conditions of Figure 2 are shown in Table 4.

Table 4. Key stream conditions based on Figure 2 (NG/BFG as heating utility case).

	Temperature (°C)	Pressure (bar)	Flow rate (kg/kg MeOH)	HHV (MJ/kg)
COG	35	1.45	0.74	32.53
CO_2	38	1.3	0.75	0
STEAM	220	1	0.47	0
SYNGAS1	800	1	1.9	17.66
SYNGAS6	240	51.95	6.81	14.01
PURGE1	45	50	0.57	11.98
EXHAUST1	1260	49.4	4.66	0.24
FLUEGAS1	615	1.1	4.66	0
FLUEGAS5	150	1.05	0.13	0
PURGE2	43	1.01	0.05	5.5
FLUEGAS3	150	1.03	4.66	0
MEOH1	241	50.95	6.81	13.6
WATER	101	1.06	0.03	0
MEOH5	56	1.01	0.97	23.3

After CO_2 recovery, the remaining BFG (Upgraded BFG: mostly CO and N_2) can be used for heat in downstream steel manufacturing processes in the same manner as the status quo without reducing its heating ability. Alternatively, the CO can also be extracted from the upgraded BFG via temperature swing adsorption (TSA). According to Ghanbari et al. [11], it is possible to extract up to 99 vol. % of CO using this method. The high purity CO can then be recycled back into the blast furnace (BF) to help reduce the coke requirement. However, the investigation of these options is out of the scope of this study.

In order to maximize MeOH production, the system optimization tests considered the flow rates of the feed stream BFG and COG, the steam to the LTWGS (if applicable), the amount of CO_2 removed (if applicable), and the integration of heating and cooling utilities. The heating utility from flue gas and MeOH exothermic reaction are used to generate high-pressure steam, while the power generated by the gas turbine is internally used for compressors and pumps. Heat that cannot be used in this process is used to generate steam utilities with various pressure levels, with heating being provided by NG. However, as specified above, the proposed CSR unit can be heated using NG, COG, or BFG.

2.6. Economic analysis

All of the economic analysis in this work is based on a plant that is the size of AMD, which means that all of the COG produced at AMD's plant will be considered usable for MeOH production. A capital cost analysis was performed using Aspen Economics v10 (AEv10) and equipment cost equations taken from Seider et al. [50] and Towler et al. [51]. Associated utility costs were calculated using Aspen Economics v10. For the Rectisol process, fixed capital costs and operation costs are linearly correlated to amount of recovered H_2S [20]. Similarly, the CO_2 recovered from the BFG is linearly correlated to the total amount of CO_2 recovered. This relationship was detailed in Section 2.1. All costs are converted to 2018 via CEPCI. Detailed calculation methods for the equipment are shown in Table 5.

Table 5. Equipment purchase costs and calculation methods

	Equipment type	*Equipment cost ($)*[1]	*Reference*
HEAT4	Fired heater for steam boiler	241,300	[50]
PREHEAT	HX-Plate and frame	450,100	[50]
DRYREFORM	Box type furnace,316S	3,170,800	Aspen Economizer
HEAT3	Floating head shell and tube[2]	398,400	[51]
MTH2SR	Vertical, cs[3] pressure vessel	43,300	[51]
COOL1	Floating head shell and tube	184,900	[51]
COMP1	Centrifugal compressors[4]	11,355,500	[50], [51]
PUMP1	Single-stage centrifugal pumps	12,200	[51]
HEAT2	Floating head shell and tube	47,200	[51]
HEAT1	Floating head shell and tube	44,800	[51]
SYN-MEOH	Fixed tube, float head, u-tube HX	1,906,200	Aspen Economizer
COOL2	Floating head shell and tube	503,600	[51]
FLASH1	Vertical, cs pressure vessel	73,200	[51]
COMP2	Centrifugal compressors + MOTOR	1,657,500	[51]
FLASH2	Vertical, cs pressure vessel	75,200	[51]
MEOH-PURIFY	Distillation column[5]	263,100	Aspen Economizer
STACK	Fired heaters for steam boiler	72,700	[50]
COMP3	Centrifugal compressors	9,414,200	[51]
GT	Gas turbine with a combustion chamber	11,117,900	Aspen Economizer

Note: [1] the equipment costs are based on using NG as a utility, without WGS
[2] Heat exchange area derived from Aspen Plus
[3] cs means carbon steel
[4] The compressor is driven partially by GT and partially by motor
[5] the cost includs distillation tower, condenser, reboiler and reflux pump

The catalysts used in the process are also estimated. Ni-MgO-$Ce_{0.8}Zr_{0.2}O_2$ was used as a catalyst in CSR [19] and was prepared using a one-step co-precipitation method. In accordance with Jang's study [19], stoichiometric quantities of $Ni(NO_3)_2{\cdot}6H_2O$, $Mg(NO_3)_2{\cdot}6H_2O$, $Ce(NO_3)_3{\cdot}6H_2O$, and ZrO_2 were purchased for catalyst preparation and sized up for their study.

The prices of the catalysts are based on the upper bounds of the listed prices. Most of the commercialized catalysts for MeOH synthesis have a lifetime of 1 to 5 years [52]. We assume that the copper-based catalyst has a lifetime of 1 year, and assume that the catalyst lifetime for the CSR unit is the same as MTH2SR, which is 4000 h due to sulfur deactivation. Since all of these catalysts can be regenerated after their lifetime, the initial catalyst costs can be included as part of the fixed capital cost.

Table 6. Catalyst price from Alibaba

	Price	Unit	Purity (%)	Reference
$Ni(NO_3)_2{\cdot}6H_2O$	100-5000	$/tonne	98	[53]

$Mg(NO_3)_2 \cdot 6H_2O$	200-300	$/tonne	>98	[54]
$Ce(NO_3)_3 \cdot 6H_2O$	3-20	$/kg	95.95-99.99	[55]
ZrO_2	20-50	$/kg	99.99	[56]
Fe_2O_3	600-1000	$/tonne	99.9	[57]
CuO	8950-9600	$/tonne	96-98	[58]
ZnO	150-300	$/tonne	95	[59]
Al_2O_3	660-830	$/tonne	93	[60]
SiO_2	1-100	$/ kg	99.8	[61]

Fe_2O_3 was used as a desulfurization catalyst for the middle-temperature sulfur-removal unit. This catalyst costs between $600 and $1000/tonne with a purity of 99.9% [57]. Supposing the size of the MTSR is linearly correlated to the amount of H_2S to be removed, the industrial sizes provided by Li [16] would require 158.4 m^3 of catalyst for 7.1 kg H_2S/h of sulfur removal. The catalyst lifetime is about 4000 hrs. In this study, the H_2S flow rate after CSR was about 13.7 kg H_2S/h. Hence, the catalyst occupied about 304.0 m^3. The catalyst density was 5.24 g/cm^3, assuming a bed voidage of 0.1. The total catalyst required for this process was about 2867.7 tonne/yr, with a maximum cost of 2.8 million $/yr.

The copper-based catalyst is most commonly used for the MeOH synthesis process. According to Lee [52], the composition of this catalyst is CuO: ZnO: Al_2O_3: SiO_2 at 55:36:8:1, respectively (page 90). The packed-bed particle density for this study was 1775 kg/m^3. The reactor was designed to contain 1000 tubes measuring 30 meters in length and 7.62 cm (3 inches) in diameter. Bed voidage is 0.1. Thus, the total reaction volume was 136.8 m^3 and the catalyst amount was 242.84 ton. Industrial-grade prices for the catalysts are shown in Table 6.

The net present value (NPV) is used to measure the profitability of this MeOH process. A cash flow analysis is applied since this process has a saleable product of MeOH subject to taxation when gross income is positive. Detailed cash flow parameters are shown in Table 7.

Table 7. Cash flow calculation parameters.

Parameters	Value	References
Depreciable percentage (%)	90	
Depreciation time (years)	7	[50]
TFCI paid by loan (%)	50	[62]
TFCI paid by equity (%)	50	[62]
Loan interest rate (%)	9.5	[62]
Loan lifetime (years)	10	
Equity interest rate (%)	15	[3]
Plant lifetime (years)	30	[3]
Inflation rate for sale (%)	3	
Inflation rate for production cost (%)	4	

Total fixed capital investment (TFCI) is calculated based on the equipment purchase cost (Table 5) and the other associated costs, such as shipping, installation, construction, contractor engineering, piping, land, royalties, start-up, and depreciation. The associated costs are calculated using the same method that was documented in the Supporting Information of Deng and Adams' [3] previous paper. The same manner, total production cost (TPC), which includes operation costs, maintenance costs, operating overhead cost, property taxes and insurance, and general expenses, is also calculated using the method detailed by Deng and Adams [3]. For conveniences purposes, both TFCI and TPC calculation methods are shown in the Appendix Table A1 and Table A2 respectively.

In addition, for conservative purposes, for cases in which the amount of electricity generated is less than the amount of electricity generated by COG combustion in the status quo case, it is assumed that difference in electricity is purchased from the grid at the industrial electricity price and this is counted as a production cost. The net effect is that the COG+BFG to MeOH retrofit cases can result in either reduced or increased CO_2 emissions compared to status quo depending on the carbon intensity of the local power grid. Likewise, the carbon credit/tax is counted as either a cost (in the case of higher carbon emissions compared to the status quo) or revenue that is untaxable (in the case of lower carbon emissions). The tax loss carry forward is also applied in the cash flow calculation. The payback period is counted from the first year until cumulative present value is positive.

With regards to CO_2 emissions, the proposed MeOH synthesis process not only accounts for the amount of carbon in the COG, but it also accounts for the carbon footprint created by the utilities that are used in the process. The cost of CO_2 avoided (CCA) in this process is calculated in the same manner detailed in [3]. Briefly, CCA is calculated as the amount of NPV gained divided by amount of CO_2 emission reduced:

$$\mathrm{CCA} = \frac{NPV_{SQ} - NPV_{MeOH,without\ CO_2\ credit}}{(CO_2\ emission\ in\ status\ quo - CO_2\ emission\ in\ MeOH) \times plant\ lifetime}\ (\$/\mathrm{tonne CO_2 e}) \quad (\mathrm{Eq.}\ 1)$$

where subscripts SQ and MeOH indicate status quo and the proposed MeOH production process. The status quo is our comparison base, which means $NPV_{SQ} := 0$.

3. Results and discussion

3.1. CSR based methane reforming and sulfur removal

The CSR units not only convert 97.8 % methane, but they also converted organic sulfur into H_2S. The R ratio is adjusted via manipulate the CO_2, steam and methane molar ratio. The detailed results and analysis of CO_2 and steam injection molar ratio to MeOH production rate are shown in the following section. In addition, for transparency and reproducibility purposes, the Aspen Plus simulation files, MATLAB code, and Microsoft Excel files used in the analysis are uploaded in the Living Archive for Process Systems Engineering repository (http://PSEcommunity.org/LAPSE:2019.0444)

3.2. Process Comparison

First, the four different processes, namely, COG utility based process without WGS (uCOG), BFG utility based process without WGS (uBFG), NG utility based process without WGS (uNG), and NG utility based process with WGS (uNG-WGS), need to be optimized and compared under these conditions so that one can be selected. In this work, the optimization objective is maximum MeOH production. The processes were optimized by varying the feed flow rate of steam and CO_2 to CSR. These optimized flow rates were determined using optimization and sensitivity analysis methods in Aspen Plus. Figure 3 shows the relationship between the variables of steam and CO_2 flow rate, and how they affect the MeOH production flow rate.

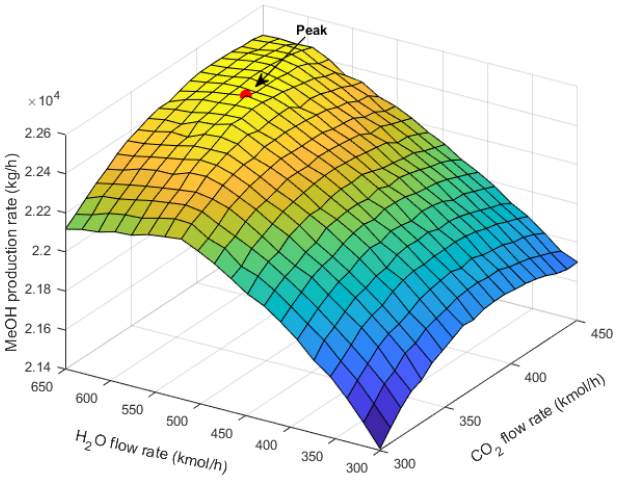

Figure 3.Sensitivity analysis of MeOH production rate with CO_2 and H_2O flow rate changes: without WGS

Along with H_2O, CO_2 is a necessary carbon resource to reduce the H_2 ratio in the syngas. As described in Section 2.2.1, H_2O is added to help increase the conversion rate of CH_4. If H_2O is not added, solid carbon will form when the CO_2 flow rate is lower than 300 kmol/h. This carbonation will not only deactivate the catalyst, but it will also reduce the carbon efficiency (defined as the number carbon atoms in the methanol divided by the number of carbon atoms in the input stream BFG and COG). In the present system, no carbon deposition will occur with a higher H_2O mole flow rate, but the R ratio will be much higher than required 2.04. This means that maximum MeOH production will likely not be achieved by decreasing the CO_2 flow rate and increasing the H_2O flow rate. Hence, the CO_2 flow rate should be higher than 300 kmol/h. Figure 3 shows that, as the CO_2 flow rate increases from 300 to 450 kmol/h, MeOH production increases and then decreases. When the H_2O flow rate is increased, MeOH production increases sharply to the maximum before slowly decreasing. The red point marked in the figure denotes the point of maximum MeOH production. At this point, the CSR reforming unit has an input gas content consisting of CH_4: CO_2: H_2O: CO: N_2: H_2: O_2: C_2H_2: HC_A with mole ratios of 1: 1.16: 1.8: 0.20: 0.41: 2.26: 0.03: 0.08: 0.16, respectively. Under this optimized CSR reforming condition, the mole fraction of the syngas mixture entering the MeOH synthesis unit (in stream SYNGAS6) contains 53.27 %, 18.78 %, 11.35 %, and 0.23 % of H_2, CO, CO_2, and H_2O, respectively. Furthermore, the H_2: CO mole ratio is 2.84, and the R parameter is equal to 1.39.

For the process that includes the WGS reaction and an additional CO_2 removal process (shown in Appendix Fig 1), the optimized CH_4: CO_2: H_2O: CO: N_2: H_2: O_2: C_2H_2: CH_A mole ratio for the CSR unit is equal to 1: 1.33: 1.69: 0.20: 0.41: 2.26: 0.03: 0.08: 0.16, respectively. After the CO_2 has been removed from the SYN-MEOH input stream, the mole fraction of the main reaction components, H_2, CO, CO_2, and H_2O, is adjusted to 55.17 %, 20.71 %, 5.91 %, and 0.10 %, respectively, for MeOH synthesis. The H_2: CO mole ratio is decreased to 2.66, while the R parameter is increased from 1.39 to 1.85. The following economic analyses are based on the corresponding optimized conditions for maximizing MeOH production.

3.2.1. Energy conversion analysis and results

Throughout the process, waste thermal energy is recovered either by the generation of utility steam (which in our analysis is credited as a saleable by-product) or as electricity in a gas turbine. Some thermal energy is lost as heat in the flue gas or as pressure drop in the various process units. The overall Sankey energy flow diagram that represents the version of the COG+BFG to MeOH process using NG as the heating utility in the CSR without WGS (the uNG case) is shown in Figure 4. The Sankey diagrams for the other process variants are quite similar and so are not shown. The uBFG and uCOG cases look very similar except the Natural Gas box is relabeled BFG for the uBFG case and the Natural Gas box does not exist for uCOG case, with similar numbers throughout.

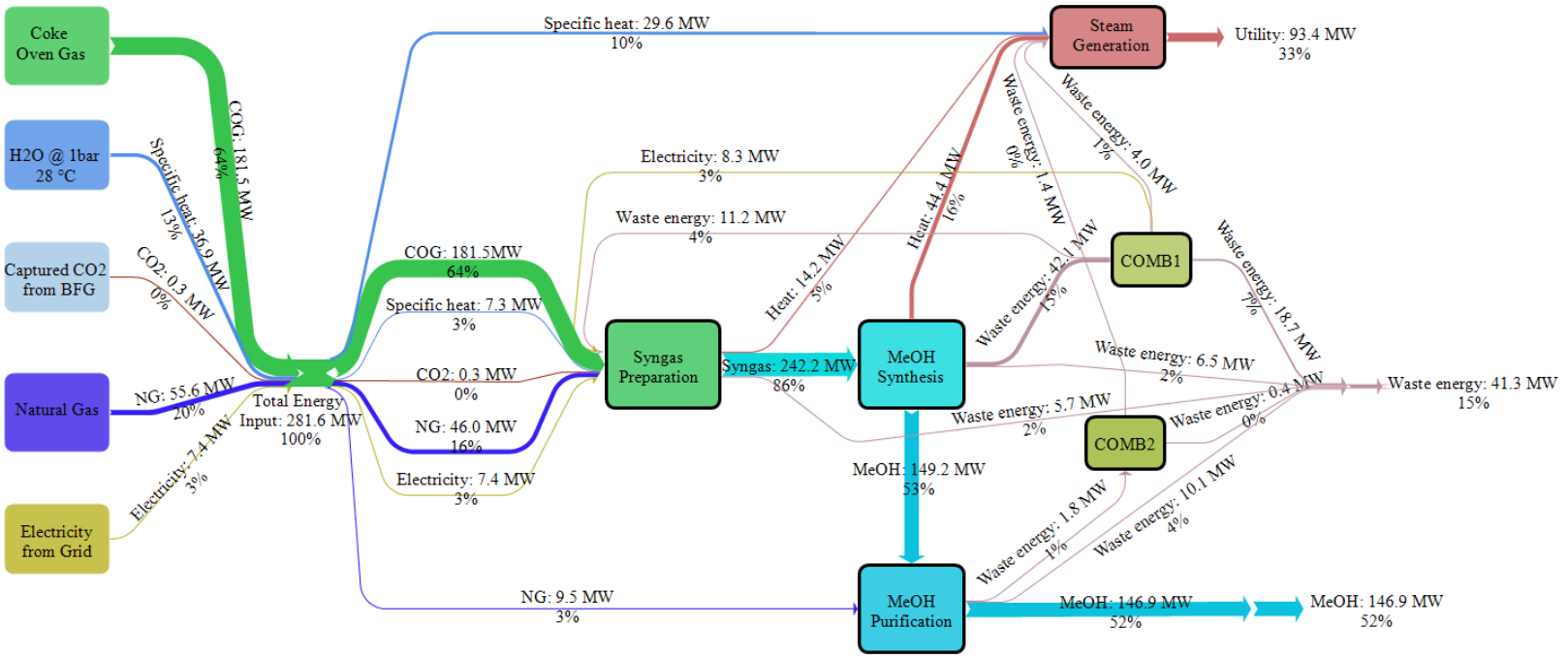

Figure 4. Sankey energy flow diagram for the COG+BFG to MeOH process with NG as heating source (without WGS) for CSR. The stream energy values are the sum of the higher heating value of the stream (for combustible streams), electric power (for electricity streams), potential energy content (for streams above atmospheric pressure), and latent/specific heats above ambient temperature.

For the uNG case, the total energy flow into the system is about 282 MW_{HHV}. This is the sum of the HHV of the COG and natural gas feeds, the electric power input from the grid, the energy associated with the captured CO_2 plus the HHV of the small amount of H_2 and CO captured along with it, and the specific heat of feed water which is slightly above ambient temperature. About 86% of this energy is retained in the syngas after the syngas preparation step, which includes the sulphur removal, methane reforming, and syngas compression steps. Only a small amount of energy is lost during syngas preparation as waste in the form of pressure losses, thermal losses through the stack, or lost in the energy content of the captured sulfur (in an amount of about 2% of the system feed), with the majority (14.2 MW) of waste heat recovered as steam for sale.

In the MeOH synthesis process about 61% of the energy in the syngas is converted to methanol. Only a small amount of energy is lost during methanol purification, resulting in a total of 52% of the system input energy recovered in the form of methanol. The total waste energy, which includes the energy lost in the flue stack, pressure drops in the reactor and other system components, air cooling in the multistage compressor, and waste water, adds up to about 15% of the total system input. The remaining energy is captured and either converted to electricity and heat (which is recycled internally to the syngas preparation step) or saleable steam. A net 33% of the original energy content of the system input is converted to saleable steam.

In this paper we define the system efficiency for each system as the total amount of energy of the primary products divided by total amount of energy input into the system:

$$\eta_{sys} = \frac{E_{MeOH,HHV} + E_{Electricity,net\_output}}{E_{COG,HHV} + E_{NG,HHV} + E_{CO_2,HHV} + E_{electricity,input} + E_{H_2O,specific\ heat}} \text{ (Eq. 2)}$$

In the above equation, η_{sys} denotes the system efficiency, $E_{MeOH,HHV}$ denotes the amount of energy fixed in product MeOH (HHV basis), and $E_{Electricity,net\_output}$ is the net electricity produced by the system. Note that $E_{Electricity,net\_output}$ is zero for all of the COG+BFG to MeOH systems in this work because they have a net consumption of electricity rather than production. It is included for comparison purposes with previously-published COG-to-electricity production systems as described in the next section. Also, note that $E_{CO_2,HHV}$ is small because only the small amounts of H_2 and CO captured along with CO_2 have a heating value.

We also define the thermal efficiency η_{therm} similarly:

$$\eta_{therm} = \frac{E_{MeOH,HHV} + E_{Electricity,net\_output} + E_{Steam}}{E_{COG,HHV} + E_{NG,HHV} + E_{CO2,HHV} + E_{electricity,input} + E_{H_2O,specific\ heat}} \text{ (Eq. 3)}$$

which includes the energy of the saleable steam produced as a by-product E_{Steam} (in terms of latent heat content). For example, in Figure 4, η_{sys} is about 52%$_{HHV}$ and η_{therm} is about 85%$_{HHV}$.

We define the system exergy efficiency (ψ_{sys}) and thermal exergy efficiency (ψ_{therm}) analogously:

$$\psi_{sys} = \frac{Ex_{MeOH} + Ex_{Electricity,net\_output}}{Ex_{COG} + Ex_{NG} + Ex_{CO2} + Ex_{electricity,input} + E_{H_2O,specific\ heat}} \text{ (Eq. 4)}$$

$$\psi_{therm} = \frac{Ex_{MeOH} + Ex_{Electricity,net\_output} + Ex_{Steam}}{Ex_{COG} + Ex_{NG} + Ex_{CO2} + Ex_{electricity,input} + E_{H_2O,specific\ heat}} \text{ (Eq. 5)}$$

Where *Ex* is the exergy of the associated stream. For this analysis, we use the following molar chemical exergies relative to atmospheric conditions (25°C, 1 bar, 60% relative humidity) [63]: methanol, 720 kJ/mol; hydrogen, 236.1 kJ/mol; methane, 831.2 kJ/mol; ethane, 1500 kJ/mol; carbon dioxide, 20 kJ/mol; carbon monoxide, 274.7 kJ/mol; liquid water, 1.3 kJ/mol; water vapour, 9.5 kJ/mol. For the steam and electricity streams, we use the exergy grade function approach:

$$Ex = E\ R \text{ (Eq. 6)}$$

Where *E* is the energy content of the stream and *R* is the exergy grade function. For electricity, *R*=1, and for steam pressures of 9 bar, 34 bar, and 40 bar, *R*=0.255, 0.338, and 0.432, respectively [64]. The resulting system and thermal exergy efficiencies of the uNG process are 62.2 % and 76.1 %, respectively.

3.2.2. Economic analysis results

TPC, TFCI, NPV, payback period, and CO_2 emission reduction, among others, were selected as the main criteria to be considered when choosing among the four processes. As Figure 5 shows, TPC consists of seven main components: utility, operations, maintenance, operation overhead, property taxes and insurance, depreciation, and general expenses. Maintenance costs were the greatest expense in all four cases, mainly due to high total depreciable costs. Furthermore, the process that uses BFG/NG as heating utility had a relatively higher utility cost than the process that uses COG. In addition, processes that incorporate WGS and CO_2 removal will have higher

maintenance and utility costs than those that do not. Detailed percentages for each cost category are shown in Figure A2 to Figure A4 in the Appendix.

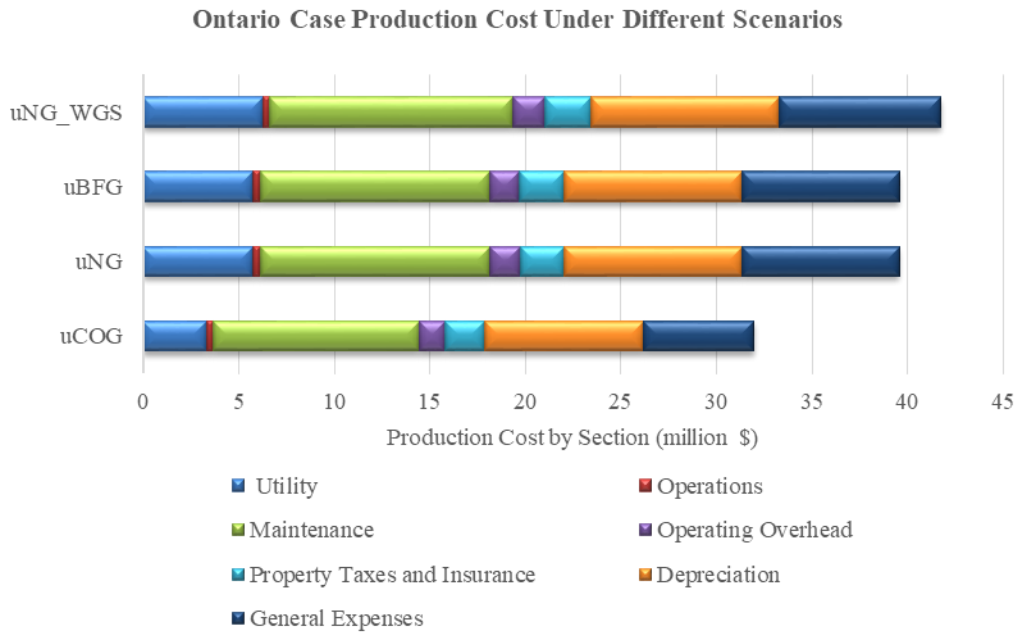

Figure 5. TPC of AMD by section, Ontario case in 2018

Table 8 provides a further detailed process comparison. As can be seen, NG/BFG is the most economical and environmental friendly heating utility, and it also produces the lowest CCA. Despite this, it should be noted that the MeOH production rate could be further increased by adding a WGS reaction process and fixing more CO_2 in the MeOH. However, the added capital costs and utility costs from such additions would outweigh the potential benefits of additional MeOH production in the Ontario case. Specifically, the inclusion of a WGS process would extend the time required to see a return on the initial investment.

Table 8. System comparison (Ontario 2018). See text for efficiency definitions.

	Status quo[a]	CCPP[b]	MeOH				*Units*
			uCOG	uNG[c]	uBFG[d]	uNG-WGS	
System efficiency (η_{sys})	15	31	52.1	52.2	52.2	52.9	$\%_{HHV}$
Thermal efficiency (η_{therm})	15	31	86.6	85.4	85.4	79.9	$\%_{HHV}$
System exergy efficiency (ψ_{sys})	-	36.7	71.3	62.2	62.2	65.7	%
Thermal exergy eff. (ψ_{therm})	-	36.7	86.1	76.1	76.1	80.3	%
Additional CO_2 consumption rate			0.23	0.28	0.28	0.23	kg CO_2/kg MeOH
MeOH conversion rate			1.09	1.35	1.35	1.37	kg MeOH /kg COG
Carbon efficiency			72.4	72.4	72.4	69.6	%
MeOH annual production rate			145	180	180	**184**	ktonne/yr
Total Production cost rate			402	366	366	371	$/tonne MeOH
Fixed capital investment	0.00	61	142	159	159	169	$M[g]
Total CO_2 emissions reduction compared to *status quo*	0.00	11	207	189	189	190	ktonne /yr
NPV	0.00	-7	-27	**21**	**21**	8	$M

NPV without carbon credit	0.00	-9	-52	-2	-2	-16	$M
Payback period	0.00	-	-	12	12	17	years
CCA		26.16	8.45	0.44	0.44	2.84	$/tonne$CO_2$e

[a]: *status quo represents the AMD, Ontario's present scenario. Which they combust COG by low pressure steam turbine to generate electricity;*
[b]: *CCPP is the scenario that proposed in the former paper [3]. It proposed a combined cycle power plant that uses the same amount of COG as status quo to produce electricity.*
[c]: *Base case.*
[d]: *assumes the use of BFG will be replaced by NG in the downstream process.*
[g]: *$M: million $.*

The methanol production processes are considerably more efficient than their electricity counterparts, with a thermal efficiency of around 85%. The difference in efficiencies between the methanol synthesis process variants is slight. Using water gas shift gives a small efficiency improvement but it is not worth the higher cost. These efficiencies are much higher than the status quo case of 15% and the CCPP case of 31%. This indicates that the proposed methanol processes do a good job of capturing and using waste heat for a saleable product. From an exergy perspective, the process using uCOG has the highest thermal exergy, while the uBFG/uNG cases have the lowest thermal exergy among methanol synthesis process. Note that high exergy efficiency does not necessary correlate with a more profitable process. On the contrary, it seems that the lower the exergy efficiency, the higher the NPV for the MeOH production system. Similarly, a direct comparison between the methanol synthesis processes and electricity production ones is not very meaningful since they produce unlike products. Instead, the comparative value between processes comes down to economic and environmental terms.

A plant of this size can produce about 145-184 ktonne of MeOH annually. Table 8 assumes that BFG will be replaced by NG in the downstream process. If surplus BFG is used for MeOH production, the downstream process will not be affected, even without other energy resource replacement. Given this, the most economical method would be to use BFG as a heating utility in CSR.

Compared to uCOG/uNG/uBFG, the uNG-WGS process had a much higher MeOH conversion rate due to R parameter adjustment; however, the use of WGS and subsequent CO_2 removal led to the lowest carbon efficiency. Without WGS and CO_2 removal, COG + BFG to MeOH has a carbon efficiency of 72.37 %.

MeOH production is more economical and environmentally friendly than both the status quo and the previously studied valorisation choice of CCPP. Despite requiring a fixed capital investment 2.6 times higher than CCPP, the production of MeOH can produce $21 million in NPV, the MeOH process consumes additional 50.4 ktonne of CO_2 and fix it into 180 ktonne of MeOH annually. It results in reducing189 ktonne of CO_2 emissions compared to the status quo, which is a 3.78 % gate-to-gate reduction in GHG emissions for the whole AMD plant (the plant emits about 5 million tonnes of CO_2 annually).

3.3. Application of this retrofit in other geological locations

As previously discussed, the base case shows that a COG+BFG to MeOH retrofit could net an extra $21 million in NPV when applied in the Ontario case. However, the effects are different if applied in other countries. Electricity (x_{Elec}) prices, electricity carbon intensity (ω_{CO_2}), MeOH market price (x_{MeOH}), location effects (purchasing power parity, or PPP), carbon taxes (T_{CO_2}), and income tax are all factors which impact both the economic and environmental bottom lines. Table 9 lists the five locations examined in this study, along with their location-related parameters.

Table 9. Location parameters at 2018.

	Ontario	USA	Finland	Mexico	China	*Reference*
PPP	1.25	1	0.88	9.04	3.54	[65]
Tax ($/tonne)	13.5	0	29.3	3.7	0	[3]
Xelec (LCU[a] ¢/kWh)	11.63	6.93	6.67	14.29	52.61	[66-71]
ω_{CO_2} (g/kWh)	40	588	285	856	1064	[3]
Xmeoh ($/tonne)	495.5	495.5	474.1	495.5	475.4	[72]
Income tax (%)	39.5	25.7	20	30	25	[73-77]
Exchange rate (LCD to USD)	1.30	1	0.85	19.23	6.62	[78]

[a]: LCU = local currency unit (Canada in CAD, USA in USD, Finland in Euro, Mexico in MXN, and China in RMB).

Since the results show that either using BFG or NG as heating utility will be the optimal choice for the COG+BFG to MeOH process, the location-based sensitivity analysis considers only cases which use NG as heating utility (the uNG design).

The results of the sensitivity analysis are summarized in Figure 6, which shows "price maps" for each of the five geographical locations. The price maps show which retrofit decision results in the highest NPV: either the construction of the COG+BFG to Methanol retrofit, the construction of the COG combined cycle power plant retrofit, or the status quo (do nothing/business as usual case). Solid lines show the boundaries of these regions using current carbon taxes for that location, and the dashed lines show the boundaries of the regions when the carbon tax is increased to $50/tonne. For context, historical market conditions are shown as circles, in which the average industrial electricity price and methanol price for a given year are shown in 2018 dollars using the inflation rate in each location [79-83]. For example, in the Finland case, if the average lifetime electricity and methanol prices are the same as they were in 2016, it would be better not to build either retrofit (i.e. the status quo case, with NPV of zero, has the highest NPV). But if they were the same as in 2010, it would be best to build the CCPP plant, and if the prices were the same as they were in 2008, it would be best to build the COG+BFG to Methanol retrofit.

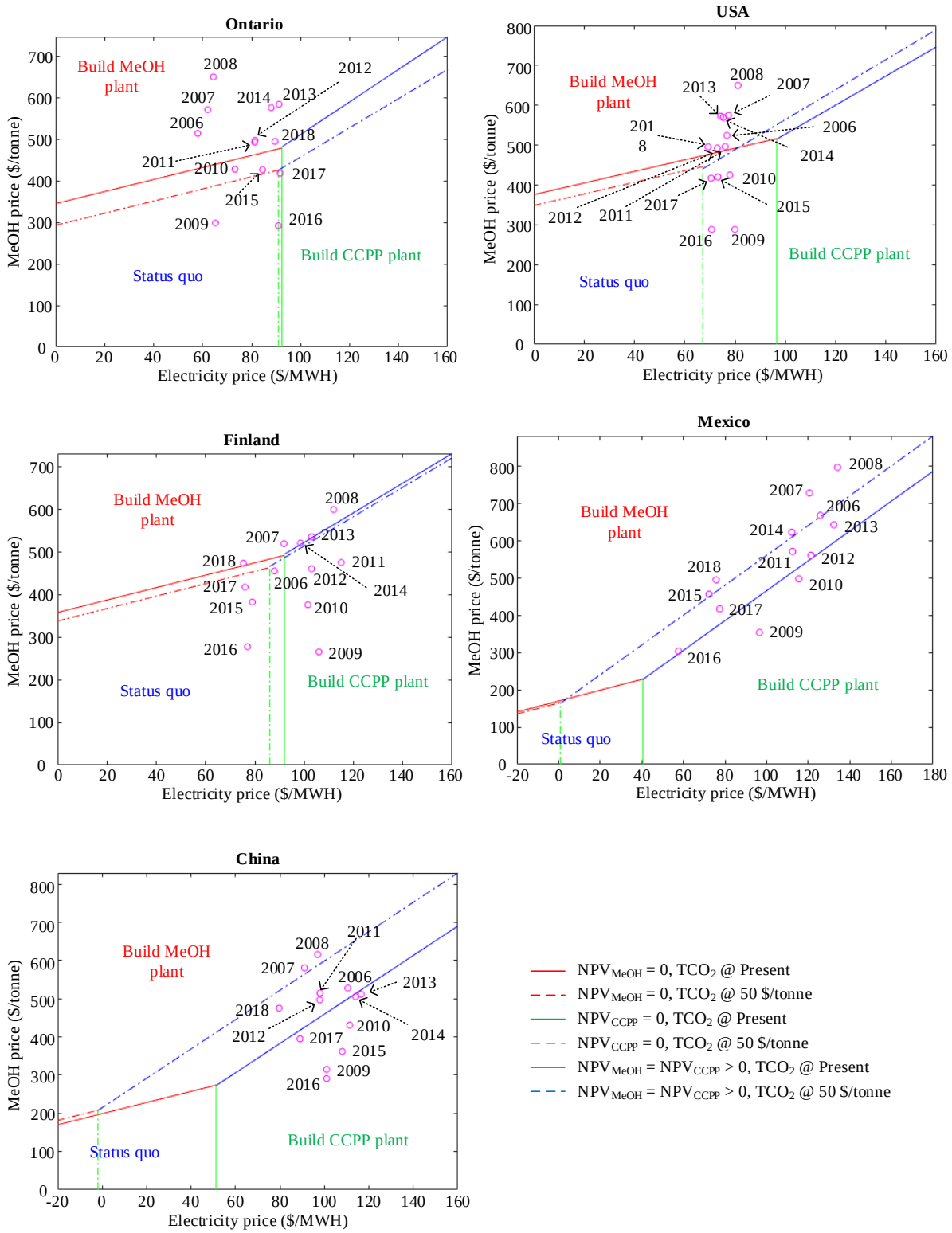

Figure 6. Price maps showing which decision results in the highest NPV based on the market conditions (namely the lifetime average electricity and methanol prices) for each of the five geographical locations of interest. Solid lines are the boundaries that separate the regions using the current carbon taxes for that region. Dashed lines are the boundaries that separate the regions when the carbon tax is increased to $50/tonne. Circles are historical average market conditions by year, converted to 2018 dollars, and are provided for context.

Figure 6 shows that the carbon tax has bigger effect for locations that have high electricity carbon intensity such as USA, Mexico and China. For the Ontario case, when carbon tax increases from present carbon tax which is about 13.53 $/ton to 50 $/ton, the decision region boundaries shift down somewhat, with almost no shifting to the left because its power grid has such a low carbon intensity. The historical data shows that the prices experienced during 8 years out of the last 13 years in Ontario would be favorable for building the MeOH plant, and this number increases to 10/13 years when carbon tax increases. Table 10 also shows that the NPV of MeOH plant is $21 million while for CCPP plant is negative $7 million at recent (2018) conditions. Though the payback period is relatively long (12 years), the amount of CO_2 emission reduced is 189 ktonne/year. For the USA, when carbon tax increases to 50 $/tonne, the NPV_{CCPP} shifts from negative to positive due to the relatively high carbon intensity of the US grid. So in the USA case, the CCPP plant should only considered with much higher carbon taxes.

Table 10. NPV of MeOH and CCPP of different locations based on location parameters in 2018

	Ontario	USA	Finland	Mexico	China
Best variants of the COG+BFG to Methanol concept					
Payback period (yrs)	12	13	18	2	2
CO_2 reduction (ktonne/yr)	189	72	137	14	-30
CCA ($/t$CO_2$e)	0.44	-10.28	7.11	-507.95	not applicable
NPV ($M)	21	22	8	220	176
NPV without carbon credit ($M)	-2	22	-29	220	176
Best variants of the COG to CCPP concept					
Payback period (yrs)	-	-	-	2	2
CO_2 reduction (ktonne/yr)	11	165	80	241	299
CCA ($/t$CO_2$e)	26.16	14.27	26.9	-11.54	-8.19
NPV ($M)	-7	-71	-43	92	74
NPV without carbon credit ($M)	-9	-71	-65	83	74
Final recommendations by region					
	Build MeOH Plant	Build MeOH Plant	Status quo or Build CCPP plant	Build MeOH Plant	Build CCPP Plant

For Finland, only five historical points are located in the Build MeOH plant region, and all of those are very close to the decision boundary. The remaining historical points are well within the status quo and Build CPPP decision regions in about equal number. Therefore, it is not clear whether it is better for them to build the CCPP plant or to do nothing. For Mexico, most of the historical points are well within the Build Methanol boundary, although the CCPP plant becomes more favorable with higher carbon taxes. Either way though, both processes are quite profitable at current conditions. For China, both CCPP and Methanol retrofit options are profitable under current conditions and historically speaking either is about as good. However, since CCPP becomes the overwhelming favorite under higher carbon taxes, and because the COG+BFG to MeOH case for China actually produces more CO_2 emissions than the status quo, CCPP is ultimately recommended for China. However, despite this, there is a very strong business case for the COG+BFG to Methanol retrofit under current market conditions in both Mexico and China.

In order to explore the uncertainties in other key parameters, a sensitivity analysis was conducted based on the Ontario 2018 base case. Fourteen parameters were each individually varied from the base case, with all else kept at their base case values, resulting in the tornado plot shown in Figure 7.

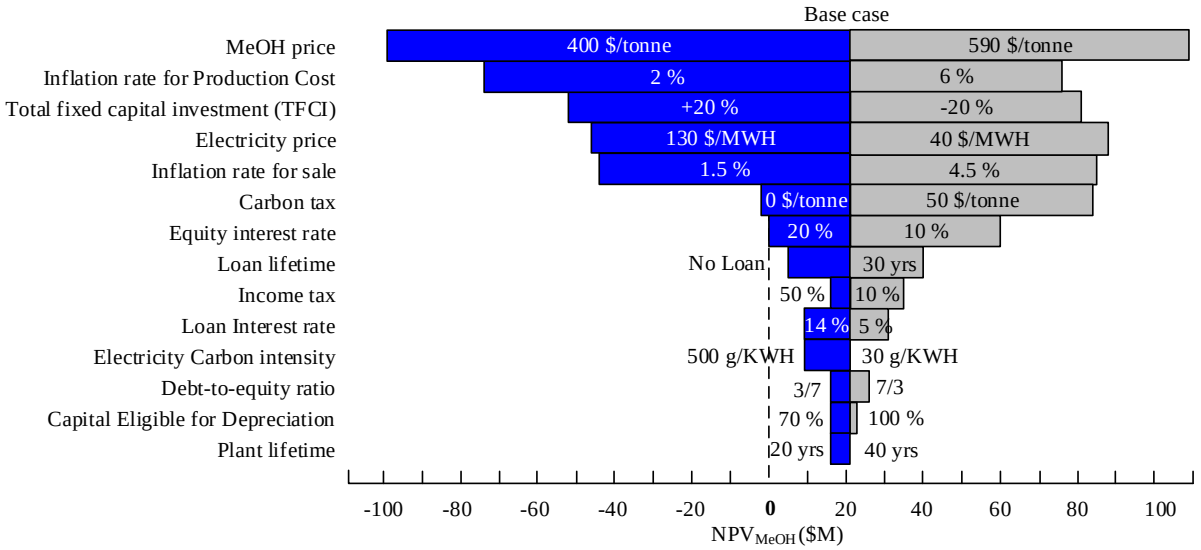

Figure 7. NPV_{MeOH} changes with uncertainties vary in certain ranges based on 2018 Ontario case

The tornado plot indicates that about ±19 % MeOH price change will cause more than 400 % of NPV increase or decrease. While about ± 2 percentage points of inflation rate for product change will cause about 260 % or 450 % NPV change. Electricity price change ± 50 % will cause NPV change about 310 %. Electricity carbon intensity and plant lifetime has relatively low impact on the NPV. (For example, when increasing plant lifetime from 30 to 40 years, the NPV almost stays the same). Debt-to-equity ratio changes ± 43 % will cause about 24 % of NPV change. Carbon tax increase 2.7 times will cause about 300 % NPV increase. Overall, this indicates that market prices and inflation tends to have a much bigger impact on the bottom line than financing details and grid intensities.

4. Conclusions

We presented a new process for converting COG and BFG to methanol that also addresses the removal of thiophene and other sulfur compounds. The proposed process drastically shortens the desulphurization process through its use of high temperature (800 °C) CO_2 steam reforming with a Ni-MgO-$Ce_{0.8}Zr_{0.2}O_2$ catalyst. In addition, this method allows the molar ratio of $(H_2-CO_2)/(CO+CO_2)$ to be adjusted by varying the CO_2 content and steam input flow rate. Significantly, the proposed COG + BFG to MeOH process is capable of producing about 180 ktonne of MeOH annually.

In terms of environmental impact, the proposed method consumes about 0.74 kg of COG and additional 0.28 kg of CO_2 per kg of methanol produced. In total, a carbon efficiency of 72.4% was achieved. Furthermore, the feasibility study conducted for AMD demonstrated that the process is efficient and results in a net CO_2 emissions reduction of 189 ktonne/yr (about 4% of net CO_2 emission reduction) and fix up to 2,970 ktonne of CO_2 into MeOH annually.

From an energy conversion aspect, CCPP has higher system efficiency than staus-quo, while COG+BFG to MeOH has the highest system efficiency among the three. About 52% of the energy in the feed is converted to MeOH, regardless of the configuration options. The energy thermal recovered in the MeOH production system (including utility recovery) adds up to 85%. This is because waste heat is very effectively used for medium pressure steam production. The thermal exergy efficiency of a processes does not necessarily have a positive correlation with thermal efficiency, and the highest thermal efficiency is not necessary the most profitable process either.

Economically, the TFCI for Ontario would be $142 million with COG as heating utility, and $159 million with BFG/NG as heating utility. TFCI is the highest when WGS is included, totalling $169 million. The payback period is 12 years when NG/BFG is used as a heating utility for Ontario. Compared to COG, BFG, and NG, the use of NG/BFG as a heating utility for CSR will yield the highest NPV for Ontario at $21 million. This is much higher than the NPV yielded by CCPP. Although the inclusion of WGS reaction produces the largest reduction in CO_2 emissions, it produces smaller economic gains compared to processes without WGS. Ultimately, the findings of this study indicate that under no circumstances is COG the best heating utility option. Compared to the status quo and the previously proposed CCPP process, generating MeOH via COG+BFG appears to be a superior option for Ontario from both an economic and environmental perspective.

Indeed, it would be highly profitable to apply this MeOH retrofit to plants Mexico and China. For Cases in which the CCA is strongly negative, such as Mexico, at 2018, it could be a potential suitable CO_2 mitigation method without requiring much policy incentives. Applications in Ontario and USA are also promising, although to a lesser degree. However, it is not recommended that Finland invest in this retrofit due to its long payback period. Ultimately, though, because of the uncertainties in future market conditions and carbon taxes (which were shown to be some of the largest influences on profitability), it is not strictly clear which design choices will be the best in any given scenario.

Although this analysis focused on steel manufacturing, there are other applications of this proposed COG+BFG to MeOH process. For example, there exist many plants which make coke from coal for purposes other than steel making. Their by-product COG utilization could also follow this retrofit route, except that the CO_2 input source might be captured CO_2 from a power plant or a cement making plant. Further, if one considers MeOH as a CO_2 storage mechanism (for example, converting the methanol into a stable solid product instead of a fuel), this route provides a potential CO_2 capture and storage mechanism in and of itself.

5. Acknowledgement

This research was funded by the Ontario Research Fund-Research Excellence Project RE09-058 and McMaster Advanced Control Consortium. We are grateful for their funding. The collaborations and data from Ian Shaw and David Meredith (AMD) and helpful conversations with Dr. Farhang Farahani (McMaster) are gratefully acknowledged.

References

[1] Worldsteel. Sustainable Steel: Indicators 2017 and the future, https://www.worldsteel.org/en/dam/jcr:938bf06f-764e-441c-874a-057932e06dba/Sust_Steel_2017_update0408.pdf; 2017 [accessed March, 2018]

[2] A. Purvis. Steel and CO_2 – a global perspecive, IEA wordshop 20th, https://www.iea.org/media/workshops/2017/ieaglobalironsteeltechnologyroadmap/ISTRM_Session1_A._PURVIS_241117.pdf; 2017 [accessed March, 2018]

[3] L.Y. Deng, T.A. Adams II. Optimization of Coke Oven Gas Desulphurization and Combined Cycle Power Plant Electricity Generation. Industrial and Engineering Chemistry Research. 57.38 (2018): 12816-12828. DOI: 10.1021/acs.iecr.8b00246.

[4] L.Y. Deng, T.A. Adams II. Methanol Production from Coke Oven Gas and Blast Furnace Gas. Computer Aided Chemical Engineering. Vol. 44. Elsevier; (2018): 163-168. https://doi.org/10.1016/B978-0-444-64241-7.50022-7.

[5] Pérez-Fortes, Mar, et al. Methanol synthesis using captured CO_2 as raw material: Techno-economic and environmental assessment. Applied Energy 161 (2016): 718-732. https://doi.org/10.1016/j.apenergy.2015.07.067.

[6] Bocin-Dumitriu A, Pérez-Fortes M, Tzimas E, Sveen T. Carbon capture and utilisation workshop. Background and proceedings. Scientific and policy report by the Joint Research Centre of the European Commission, European Commission, European Union, http://publications.jrc.ec.europa.eu/repository/handle/JRC86324; 2013 [accessed June 16th, 2019]

[7] S.H. Kim, M.S. Kim, Y.T. Kim, G.J. Kwak, J.Y. Kim. Techno-economic evaluation of the integrated polygeneration system of methanol, power and heat production from coke oven gas. Energy Conversion and Management. 182 (2019): 240-250. https://doi.org/10.1016/j.enconman.2018.12.037.

[8] Wu, Xiang, Rong Wu, and Sufang Wu. Kinetic study of reactive sorption-enhanced reforming of coke oven gas for hydrogen production. Journal of Natural Gas Science and Engineering. 27 (2015): 1432-1437. https://doi.org/10.1016/j.jngse.2015.10.007.

[9] J.M. Bermúdez, N. Ferrera-Lorenzo, S. Luque, A. Arenillas, J.A. Menéndez. New process for producing methanol from coke oven gas by means of CO_2 reforming. comparison with conventional process. Fuel processing technology. 115 (2013): 215-221. https://doi.org/10.1016/j.fuproc.2013.06.006.

[10] Yi, Qun, et al. Process development of coke oven gas to methanol integrated with CO2 recycle for satisfactory techno-economic performance. Energy 112 (2016): 618-628. https://doi.org/10.1016/j.energy.2016.06.111.

[11] H. Ghanbari, H. Saxén, I. E. Grossmann. Optimal design and operation of a steel plant integrated with a polygeneration system. AIChE Journal. 59.10 (2013): 3659-3670. https://doi.org/10.1002/aic.14098.

[12] H. Ghanbari, F. Pettersson, H. Saxen. Sustainable development of primary steelmaking under novel blast furnace operation and injection of different reducing agents. Chemical Engineering Science. 129 (2015): 208-222. https://doi.org/10.1016/j.ces.2015.01.069.

[13] Z.C. Zhao, Y.Y. Ding. Desulphurization and Purification Technology for Coke Oven Gas Synthesis into Syngas. Industrial Technology. 20 (2015): 40.

[14] A.P. Chen. Analysis on the Purification Technology of Coke-Oven Gas to Methanol. Sci-Tech Information Development & Economy. 29 (2009): 214-215.

[15] C.M. Wu. Study on Methanol Production Technology from Coke Oven Gas, Gas & Heat. 1 (2008): 36-42.

[16] J.N. Li. 焦炉煤气制甲醇生产中干法脱硫工艺的改进 (The Process Improvements of Dry Desulphurization in the Production of Coke-oven Gas-to-methanol). Sci-Tech Information development & Economy. 19.16 (2009):180-182.

[17] H.C. Cao, K.L. Bei, P.W., G.Z. Zhang, Y.F. Zhang. 焦炉煤气制甲醇工艺中的净化脱硫探讨(Discussion of the Desulphurization Process for Coke Oven Gas Synthesis to Methanol). Symposium on Methanol and Its Downstream Products New Technologies. 2007.

[18] J.M. Bermúdez, B. Fidalgo, A. Arenillas, J.A. Menéndez. Dry reforming of coke oven gases over activated carbon to produce syngas for methanol synthesis. Fuel. 89.10 (2010): 2897-2902. https://doi.org/10.1016/j.fuel.2010.01.014.

[19] Jang, Won-Jun, et al. Combined steam and carbon dioxide reforming of methane and side reactions: Thermodynamic equilibrium analysis and experimental application. Applied energy. 173 (2016): 80-91. https://doi.org/10.1016/j.apenergy.2016.04.006.

[20] Dalrymple, Dennis A., Timothy W. Trofe, and James M. Evans. Liquid redox sulfur recovery options, costs, and environmental considerations. Environmental progress. 8.4 (1989): 217-222. https://doi.org/10.1002/ep.3300080412.

[21] S. Abrol, C. M. Hilton. Modeling, simulation and advanced control of methanol production from variable synthesis gas feed. Computers & Chemical Engineering. 40 (2012): 117-131. https://doi.org/10.1016/j.compchemeng.2012.02.005.

[22] Lee, Sunggyu. Methanol synthesis technology. Florida: CRC Press. Inc.; 1989.

[23] Z.B. Yang, W.Zh. Ding, Y.Y. Zhang, X.G. Lu, Y.W. Zhang, P.J. Shen. Catalytic Partial Oxidation of Coke Oven Gas to Syngas in an Oxygen Permeation Membrane Reactor Combined with NiO/MgO Catalyst. International Journal of Hydrogen Energy. 35.12 (2010): 6239–6247. https://doi.org/10.1016/j.ijhydene.2009.07.103.

[24] W. Uribe-Soto, J.F. Portha, J.M. Commenge, L. Falk. A review of thermochemical processes and technologies to use steelworks off-gases. Renewable and Sustainable Energy Reviews. 74(2017): 809-823. https://doi.org/10.1016/j.rser.2017.03.008.

[25] Z. Qiao, X.F. She, J.S. Wang, Q.G. Xue. Current State of Gas Resource Utilization and Countermeasures of Energy Saving for Integrated Iron and Steel Works in China. Advanced Materials Research. Trans Tech Publications. 849 (2014): 165-169. https://doi.org/10.4028/www.scientific.net/AMR.849.165.

[26] H. Hell, M. Helle, H. Saxen, F. Pettersson. Optimization of top gas recycling conditions under high oxygen enrichment in the blast furnace. ISIJ international. 50.7 (2010): 931-938. https://doi.org/10.2355/isijinternational.50.931

[27] The Linde Group. Carbon dioxide recovery and removal. https://www.linde-engineering.com/en/process_plants/adsorption-and-membrane-plants/carbon_dioxide_recovery_removal/index.html; 2018 [accessed Nov., 2018]

[28] H. Kim, J. Lee, S. Lee, I.B. Lee, J. Park, J. Han. Economic process design for separation of CO_2 from the off-gas in ironmaking and steelmaking plants. Energy. 88 (2015): 756-764. https://doi.org/10.1016/j.energy.2015.05.093.

[29] Á. A. Ramírez-Santos, , C. Castel, E. Favre. A review of gas separation technologies within emission reduction programs in the iron and steel sector: Current application and development perspectives. Separation and Purification Technology. (2018). https://doi.org/10.1016/j.seppur.2017.11.063.

[30] J.A. Lie, T. Vassbotn, M.B. Hagg, D. Grainger, T.J. Kim, T. Mejdell. Optimization of a membrane process for CO_2 capture in the steelmaking industry. International Journal of Greenhouse Gas Control. 1.3 (2007): 309-317. https://doi.org/10.1016/S1750-5836(07)00069-2.

[31] F. A. Tobiesen, H. F. Svendsen, T. Mejdell. Modeling of blast furnace CO_2 capture using amine absorbents. Industrial & Engineering Chemistry Research. 46.23 (2007): 7811-7819. https://pubs.acs.org/doi/abs/10.1021/ie061556j.

[32] D. Aaron, C. Tsouris. Separation of CO_2 from flue gas: a review, Separation Science and Technology. 40.1-3 (2005): 321-348. https://doi.org/10.1081/SS-200042244.

[33] K. Goto, H. Okabe, F.A. Chowdhury, S. Shimizu, Y. Fujioka, M. Onoda. Development of novel absorbents for CO_2 capture from blast furnace gas. International Journal of Greenhouse Gas Control. 5.5 (2011): 1214-1219. https://doi.org/10.1016/j.ijggc.2011.06.006.

[34] W.J. Choi, J.B. Seo, S.Y. Jang, J.H. Jung, K.J. Oh. Removal characteristics of CO_2 using aqueous MEA/AMP solutions in the absorption and regeneration process. Journal of Environmental Sciences. 21.7 (2009): 907-913. https://doi.org/10.1016/S1001-0742(08)62360-8.

[35] A.L. Kohl, R. Nielsen. Gas purification. Elsevier: 1997.

[36] Á. A. Ramírez-Santos, C. Castel, E. Favre. Utilization of blast furnace flue gas: opportunities and challenges for polymeric membrane gas separation processes. Journal of Membrane Science. 526 (2017): 191-204. https://doi.org/10.1016/j.memsci.2016.12.033.

[37] G. Zhang, Y. Dong, M.Feng, Y. Zhang, W. Zhao, H.C.Cao. CO_2 reforming of CH_4 in coke oven gas to syngas over coal char catalyst. Chemical Engineering Journal. 156.3 (2010): 519-523. https://doi.org/10.1016/j.cej.2009.04.005.

[38] L. Hoseinzade, T. A. Adams II. Modeling and simulation of an integrated steam reforming and nuclear heat system. International Journal of Hydrogen Energy. 42.39 (2017): 25048-25062. https://doi.org/10.1016/j.ijhydene.2017.08.031.

[39] J.M. Bermúdez, B. Fidalgo, A. Arenillas, J.A. Menerdez. CO_2 reforming of coke oven gas over a Ni/γAl_2O_3 catalyst to produce syngas for methanol synthesis. Fuel. 94 (2012): 197-203. https://doi.org/10.1016/j.fuel.2011.10.033.

[40] K.Y. Koo, J.H. Lee, U.H. Jung, S.H. Kim, W.L. Yoon. Combined H_2O and CO_2 reforming of coke oven gas over Ca-promoted Ni/$MgAl_2O_4$ catalyst for direct reduced iron production. Fuel. 153 (2015): 303-309. https://doi.org/10.1016/j.fuel.2015.03.007.

[41] J.W. Moon, S.J. Kim, Y. Sasaki. Effect of preheated top gas and air on blast furnace top gas combustion. ISIJ international. 54.1 (2014): 63-71. https://doi.org/10.2355/isijinternational.54.63.

[42] A.P. Chen. 焦炉煤气制甲醇净化工艺分析 (Analysis on the purification technology of coke-oven gas to methanol). Sci-Tech Information development & Economy: 19.21 (2009): 214-216.

[43] D.L. Trimm. Catalysts for the control of coking during steam reforming. Catalysis Today. 49.1-3 (1999): 3-10. https://doi.org/10.1016/S0920-5861(98)00401-5.

[44] J.R. Rostrup-Nielsen. Sulfur-passivated nickel catalysts for carbon-free steam reforming of methane. Journal of Catalysis. 85.1 (1984): 31-43. https://doi.org/10.1016/0021-9517(84)90107-6.

[45] G.Hochgesand. Rectisol and purisol. Industrial & Engineering Chemistry. 62.7 (1970): 37-43.

[46] J.C. Elgin. II. Pure Sulfur Compounds in Hydrocarbon Materials in Contact with Nicel Catalysts. Industrial & Engineering Chemistry. 22.12 (1930): 1290-1293. DOI: 10.1021/ie50252a012.

[47] G. Liu, D. Willcox, M. Garland, H.H. Kung. The rate of methanol production on a copper-zinc oxide catalyst: The dependence on the feed composition. Journal of Catalysis. 90.1 (1984): 139-146. https://doi.org/10.1016/0021-9517(84)90094-0.

[48] Y. Yang, C.A. Mims, D.H. Mei, C.H.F. Peden, C.T. Campbell. Mechanistic studies of methanol synthesis over Cu from $CO/CO_2/H_2/H_2O$ mixtures: The source of C in methanol and the role of water. Journal of catalysis. 298 (2013): 10-17. https://doi.org/10.1016/j.jcat.2012.10.028.

[49] C.N. Hamelinck, A. P.C. Faaij. Future prospects for production of methanol and hydrogen from biomass. Journal of Power sources. 111.1 (2002): 1-22. https://doi.org/10.1016/S0378-7753(02)00220-3.

[50] W. D. Seider, J. D. Seader, D. R. Lewin, S. Widagdo. Product and process design principles: synthesis, analysis, and evaluation. 3rd ed. New York: Wiley; (2010).

[51] G. Towler, R.K. Sinnott. Chemical engineering design: principles, practice and economics of plant and process design. Chapter 7. Capital cost estimation. 2nd ed. Elsevier; 2012, p. 307-351.

[52] Lee, Sunggyu. Methanol synthesis technology. Chapter 8. Catalytic activity and life. CRC Press; (1989).

[53] [$Ni(NO_3)_2 \cdot 6H_2O$] Alibaba. 98% Nickel nitrate hexahydrate $Ni(NO_3)_2.6H_2O$. https://www.alibaba.com/product-detail/98-Nickel-nitrate-hexahydrate-Ni-NO3_507738630.html?spm=a2700.7724838.2017115.10.17a57c6aemnyHu&s=p; 2018 [accessed Oct. 9th, 2018]

[54] [$Mg(NO_3)_2 \cdot 6H_2O$] Alibaba. Magnesium Nitrate Hexahydrate 98% 99% $Mg(NO_3)_2.6H_2O$ Manufacturer Price. https://www.alibaba.com/product-detail/Magnesium-Nitrate-Hexahydrate-98-99-Mg_60404962193.html?spm=a2700.7724838.2017115.1.7fea3691lRhDg1&s=p; 2018 [accessed Oct. 9th, 2018]

[55] [$Ce(NO_3)_3 \cdot 6H_2O$] Alibaba. Cerium Nitrate $Ce(NO_3)_3.6H_2O$. https://www.alibaba.com/product-detail/Cerium-Nitrate-Ce-NO3-3-6H2O_60795755062.html?spm=a2700.7724838.2017115.1.4e2a46b4Nre28A&s=p; 2018 [accessed Oct. 9th, 2018]

[56] [ZrO_2] Alibaba. hard coating material zro_2 supplier. https://www.alibaba.com/product-detail/hard-coating-material-zro2-supplier_60797105002.html?spm=a2700.7724838.2017115.21.551d6163VZAxAc&s=p; 2018 [accessed Oct. 9th, 2018]

[57] [Fe_2O_3] Alibaba. Ferric Oxide FE_2O_3 Desulfurization Catalyst. https://www.alibaba.com/product-detail/Ferric-Oxide-FE2O3-Desulfurization-Catalyst_60780101912.html?spm=a2700.7724838.2017115.11.605115c3qq1Ueb&s=p; 2018 [accessed Sep. 27th, 2018]

[58] [CuO] Alibaba. copper oxide catalyst CUO raw material copper oxide powder. https://www.alibaba.com/product-detail/copper-oxide-catalyst-CUO-raw-material_60735971031.html?spm=a2700.7724838.2017115.1.2238590ba72ECk&s=p; 2018 [accessed Sep. 27th, 2018]

[59] [ZnO] Alibaba. zno desulfurization catalyst used in oil refinery. https://www.alibaba.com/product-detail/zno-desulfurization-catalyst-used-in-oil_60804559218.html?spm=a2700.7724838.2017115.1.72545c96TAc52x; 2018 [accessed Sep. 27th, 2018]

[60] [Al_2O_3] Alibaba. AL_2O_3 Adsorbents Activated Alumina Catalyst Desiccant. https://www.alibaba.com/product-detail/AL_2O_3-Adsorbents-Activated-Alumina-Catalyst-Desiccant_60834778470.html?spm=a2700.7724838.2017115.1.494f6cdfXQlv1h&s=p; 2018 [accessed Sep. 27th, 2018]

[61] [SiO_2] Alibaba. SiO_2 powder CAS:14808-60-7 high purity Nano Silicon Oxide Powder for chemical catalyst. https://www.alibaba.com/product-detail/SiO2-powder-CAS-14808-60-7_60585046958.html?spm=a2700.7724838.2017115.20.57441b7dXdAOw3&s=p; 2018 [accessed Sep. 27th, 2018]

[62] P. Worhach, J. Haslbeck, Recommended Project Finance Structures for the Economic Analysis of Fossil-Based Energy Projects, DOE/NETL-401/090808, September 8, 2008.

[63] Demirel, Y. Nonequilibrium Thermodynamics: Transport and Rate Processes in Physical Chemical, and Biological Systems, 3rd Ed. Chapter 4 – Using the Second Law: Thermodynamic Analysis. Elsevier: Amsterdam. 2014.

[64] Dincer I, Rosen MA. Exergy: Energy, Environment, and Sustainable Development. Elsevier: Oxford. 1st Ed. 2007.

[65] The World Bank, PPP conversion factor, GDP (LCU per international $), https://data.worldbank.org/indicator/PA.NUS.PPP; 2017 [accessed June 2nd, 2019]

[66] [Data] Average weighted hourly electricity price in Ontario from 2004 to 2018 (in Canadian dollar cents per kilowatt hour), https://www.statista.com/statistics/483230/ontario-yearly-average-electricity-market-price/; 2018 [accessed May 22nd, 2019]

[67] [Data] Global Adjustment for Mid-sized and Large Businesses, http://www.ieso.ca/en/Learn/Electricity-Pricing/Global-Adjustment-for-Mid-sized-and-Large-Businesses; 2018 [accessed May 22nd, 2019]

[68] [Data] Average U.S. retail prices of electricity between 1998 and 2018, by sector (in cents per kilowatt hour), https://www.statista.com/statistics/200197/average-retail-price-of-electricity-in-the-us-by-sector-since-1998/; 2018 [accessed May 23rd, 2019]

[69] [Data] Prices of electricity for industry in Finland from 1995 to 2017 (in euro cents), https://www.statista.com/statistics/595853/electricity-industry-price-finland/; 2018 [accessed May 21st, 2019]

[70] [Data] Precios medios de energía eléctrica por tipo de tarifa, https://datos.gob.mx/busca/dataset/precios-medios-de-energia-electrica-por-tipo-de-

tarifa?fbclid=IwAR12XrfUdQMVV4ENQxlNmXX7xNEYgo4zAxONNfuIQOfMjbDteR9c5S5dR7E; 2018 [accessed May 22nd, 2019]

[71] [Data]全国最新电价汇总, http://www.sohu.com/a/271827080_146940; 2018 [accessed May 22nd, 2019]

[72] [Data] Methanex, 2018, Methanex posts regional contract methanol prices for North America, Europe and Asia, https://www.methanex.com/our-business/pricing; 2018 [accessed April, 2018].

[73] [Data] Corporation tax rates, https://www.canada.ca/en/revenue-agency/services/tax/businesses/topics/corporations/corporation-tax-rates.html; 2018 [accessed June 12th, 2019].

[74] Kyle Pomerleau, The United States' Corporate Income Tax Rate is Now More in Line with those levied by other Major Nations. https://taxfoundation.org/us-corporate-income-tax-more-competitive/; 2018 [accessed June 12th, 2019].

[75] [Data] Finland Corporate Tax Rate, https://tradingeconomics.com/finland/corporate-tax-rate; 2018 [accessed June 12th, 2019].

[76] [Data] Mexico Corporate Tax Rate, https://tradingeconomics.com/mexico/corporate-tax-rate; 2018 [accessed June 12th, 2019].

[77] [Data] China Corporate Tax Rate, https://tradingeconomics.com/china/corporate-tax-rate; 2018 [accessed June 12th, 2019].

[78] [Data] Yearly Average rates. Historical exchange rates, https://www.ofx.com/en-ca/forex-news/historical-exchange-rates/yearly-average-rates/; 2018 [accessed May 23rd, 2019]

[79] [Data] Inflation calculator, https://inflationcalculator.ca/ontario/; 2018 [accessed June 5th, 2019]

[80] [Data] US Inflation Calculator, https://www.usinflationcalculator.com/; 2018 [accessed June 5th, 2019]

[81] [Data] Inflation calculator for Finland, https://www.worlddata.info/europe/finland/inflation-rates.php;

[82] [Data] Calculate Price change due to inflation for custom period, https://www.statbureau.org/en/mexico/inflation-calculators?dateBack=2017-12-1&dateTo=2018-7-1&amount=75.76; 2018 [accessed June 5th, 2019]

[83] [Data] Inflation calculator-Chinese Renminbi, https://www.inflationtool.com/chinese-renminbi?amount=388&year1=2017&year2=201; 2018 [accessed June 5th, 2019]

Appendix

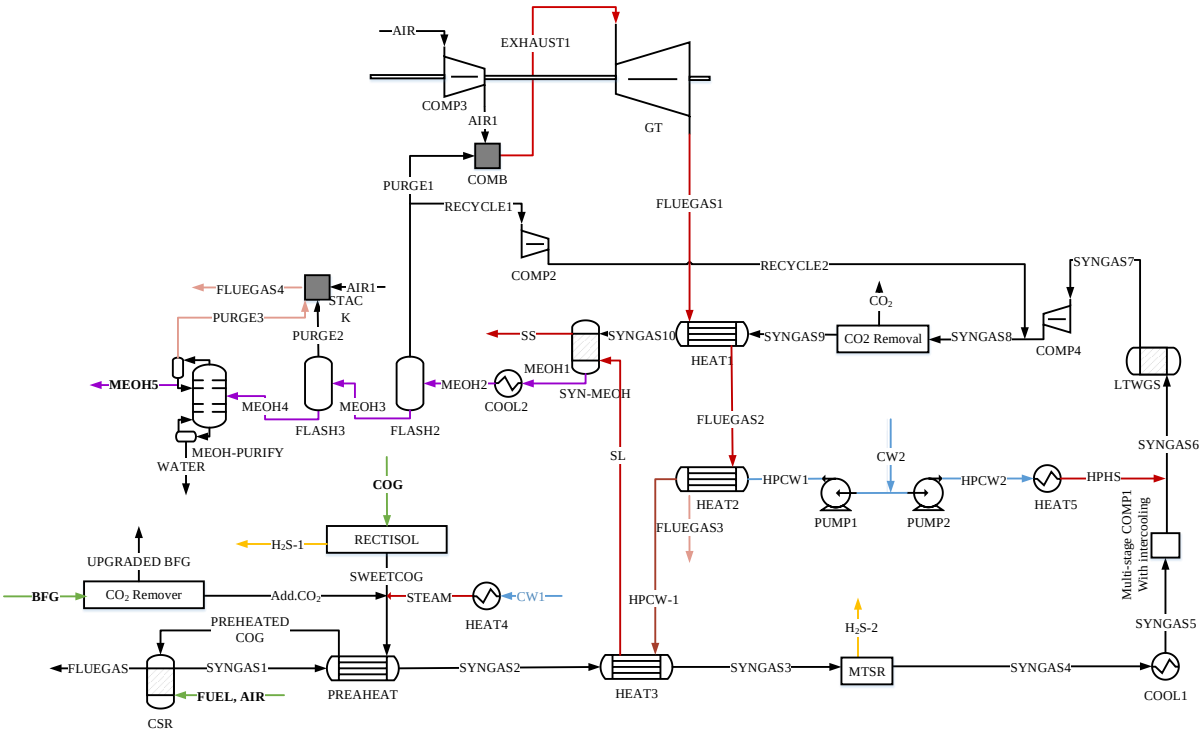

Figure A1. Proposed COG+BFG to MeOH with WGS

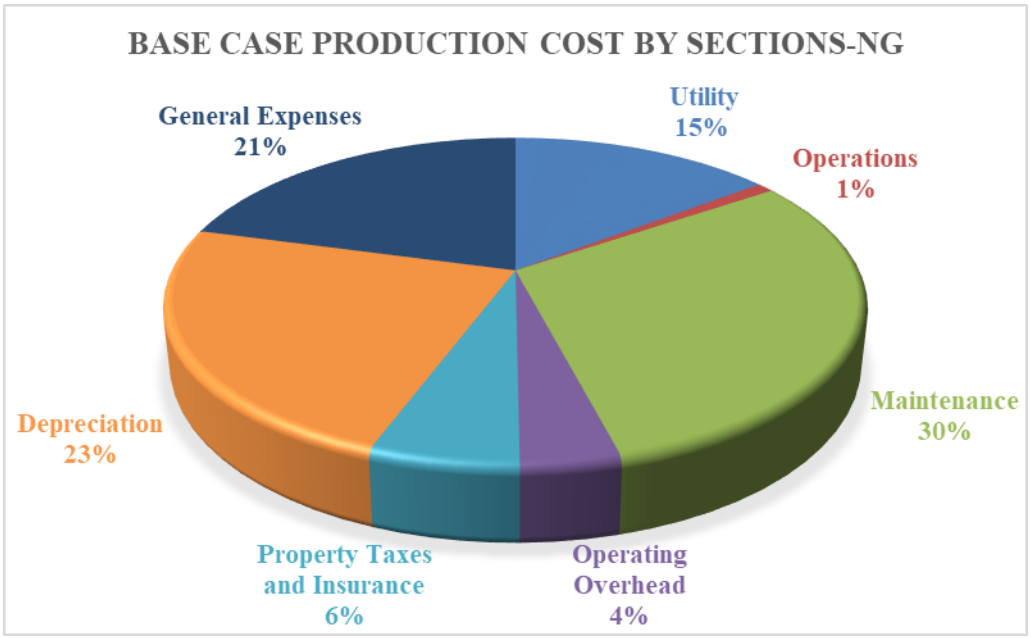

Figure A2. Production cost share with NG/BFG as heating utility without WGS

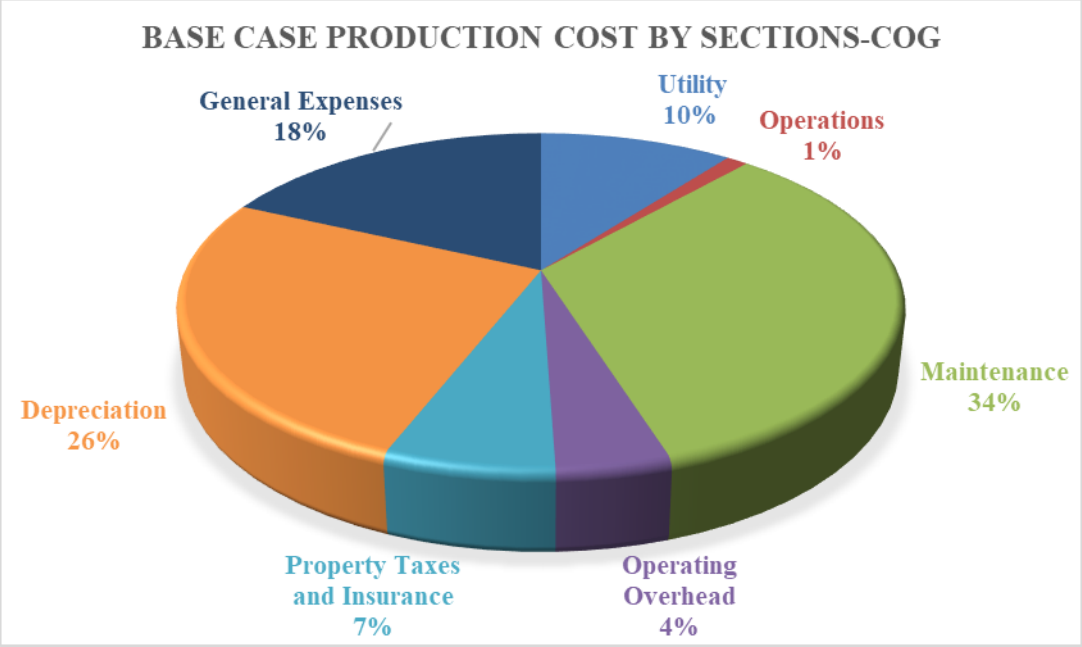

Figure A3. Production cost share with COG as heating utility without WGS

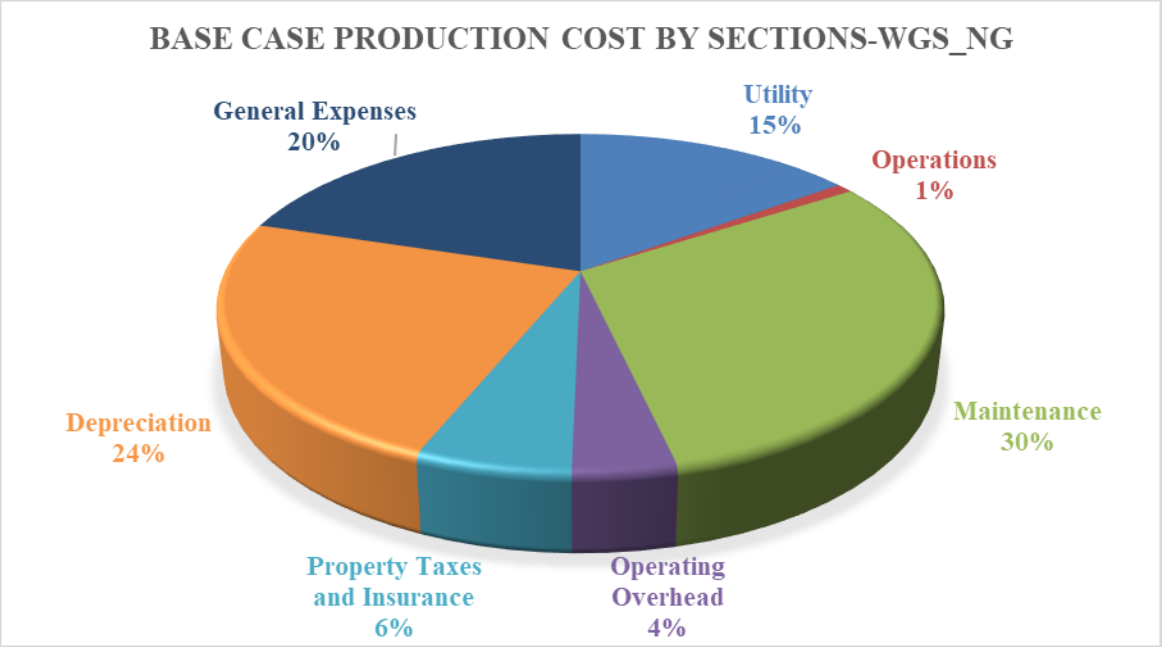

Figure A4. Production cost share with NG as heating utility with WGS

Table A1. Factors for total capital investment calculation [50]

F.O.B. (Purchase) Costs	C_{fob}	Historical charts
Installation Costs	C_{inst}	$0.714*C_{fob}$
Construction Costs (Incl. Labor)	C_{cons}	$0.63*C_{fob}$
Total Direct Costs	C_{TDC}	$C_{TDC}=C_{fob} + C_{inst} + C_{cons}$
Shipping (Incl. Insurance & Tax)	C_{ship}	$0.08*C_{fob}$
Construction Overhead	C_{over}	$0.571*C_{fob}$
Contractor Engineering	C_{engn}	$0.296*C_{fob}$

Contingencies	C_{slop}	0.15 - 0.35*C_{fob}
Total Indirect Costs	C_{TIC}	$C_{TIC}=C_{ship}+C_{over}+C_{engn}+C_{slop}$
Total Depreciable Capital	C_{dep}	$C_{dep}=C_{TDC}+C_{TIC}$
Land (Pure Real Estate)	C_{land}	0.02*C_{dep}
Royalties	C_{royle}	0.02*C_{dep}
Startup Costs	C_{strt}	0.02-0.3*C_{dep} (often 0.1)
Fixed Capital Investment	C_{FCI}	$C_{FCI}=C_{dep}+C_{land}+C_{royle}+C_{strt}$
Cash Reserves	C_{cash}	8.33% of total annual expense
Inventory	C_{inv}	1.92% of annual tangible sales
Accounts Receivable	C_{recy}	8.33% of total annual revenue
Accounts Payable	C_{payb}	8.33% of annual tangible expenses
Total Working Capital	C_{wc}	sum of this section 0.7-0.89*(C_{fob}+C_{ship})
Total Capital Investment	C_{TCI}	(total FCI and working capital) $C_{TCI} = C_{FCI}+C_{WC}$

Table A2. Factors for total production cost calculation [50]

Annual operation (hr) 8000			
Operations (labor-related)			*463800*
Direct wages and benefits (DW&B)	35	$/hr	*280000*
Direct salaries and benefits	15	% of DW&B	*42000*
Operating supplies and services	6	% of DW&B	*16800*
Technical assistance to manufacturing			*60000*
Control laboratory			*65000*
Maintenance (M)			
Wages and benefits (MW&B)	13	% of C_{TDC}	
Fluid handling process	3.5	% of C_{TDC}	
Salaries and benefits	25	% of MW&B	
Materials and services	100	% of MW&B	
Maintenance overhead	5	% of MW&B	
Operating overhead			
General plant overhead	7.1	% of M&O-SW&B	
Mechanical department services	2.4	% of M&O-SW&B	
Employee relations department	5.9	% of M&O-SW&B	
Business services	7.4	% of M&O-SW&B	
Property taxes and insurance	2	% of C_{TDC}	
Depreciation			
Direct plant	8	% of (C_{TDC}-1.18 C_{alloc})	
Allocated plant	6	% of 1.18 C_{alloc}	
Rental fees			
Licensing fees			
Cost of Manufacture (COM)	the sum of the above from DW&B		
General Expenses			
Selling (or transfer) expense	3	% of sales	

Direct research	4.8	% of sales
Allocated research	0.5	% of sales
Administrative expense	2	% of sales
Management incentive compensation	1.25	% of sales
Total general expenses (GE)		
Total Production cost (C)	TPC = COM+GE	